

ON A THREE DIMENSIONAL VISION BASED COLLISION AVOIDANCE MODEL

CÉLINE PARZANI AND FRANCIS FILBET

ABSTRACT. This paper presents a three dimensional collision avoidance approach for aerial vehicles inspired by coordinated behaviors in biological groups. The proposed strategy aims to enable a group of vehicles to converge to a common destination point avoiding collisions with each other and with moving obstacles in their environment. The interaction rules lead the agents to adapt their velocity vectors through a modification of the relative bearing angle and the relative elevation. Moreover the model satisfies the limited field of view constraints resulting from individual perception sensitivity.

From the proposed individual based model, a mean-field kinetic model is derived. Simulations are performed to show the effectiveness of the proposed model.

KEYWORDS. collision avoidance, Individual-based models.

CONTENTS

1. Introduction	1
2. Agent-based model for collision avoidance	3
2.1. Perception Phase	3
2.2. Decision Making Phase	6
2.3. Avoidance of obstacles and influence of the target	13
2.4. Influence of the noise	14
2.5. Agent-based model for collision avoidance	14
3. Mean field kinetic model	14
3.1. Mean field model without noise	15
3.2. Mean field model with noise	17
4. Numerical experiments	18
4.1. Collision avoidance in the horizontal plane	18
4.2. Influence of the vision cone	18
4.3. Collision avoidance in 3D	19
4.4. Moving around obstacles	20
5. Conclusion and Perspectives	22
6. Acknowledgement	22
References	22

1. INTRODUCTION

In this paper we are interested in swarm modelling which represents the collective behavior of interacting agents of similar size and shape such that insects, birds or aerial vehicles. Inside the swarm, agents communicate with each other, working together to accomplish tasks and reach goals. As an example, in the last few years, the use of unmanned aerial vehicles swarm has been widely developed for numerous applications including monitoring of natural disasters, industrial accidents, surveillance of crowds, sensing in large environments, search and rescue missions, searching for sources of pollution, closed observation of protected areas and many others (see for instance [25] or [23]). Main advantages are that the considered swarm can cover quickly a large area only requiring one operator or can scan high-risk sites rapidly whereas large vehicle cannot. All of these real-world challenges motivate serious

investigations on how to control multiple vehicles cooperating automatically to accomplish a given task.

On the other hand, nature provides great examples of decentralized, coordinated behaviors in groups of living organisms. Indeed, it is surprising how swarms of insects or flocks of birds can travel in large, dense groups without colliding (see [2, 3, 19] and [29]). Even in the presence of external obstacles these agents are able to avoid collisions smoothly and such biological groups are remarkably effective at maintaining optimized group structure, detecting and avoiding obstacles and predators, and performing other complex tasks. Observing animals or pedestrians collective motion, remarkable patterns are achieved by following simple rules. Such impressive inter-agent coordination is accomplished despite their natural physiological constraints. Although individual agents have limited sensing capability and cannot see the whole formation, they can form a flock with no apparent leader, which implies the lack of a centralized command. This highly coordinated collective behavior emerges from localized interactions among individuals within the swarm.

In this context, the objective of this paper is to propose a three dimensional model for a swarm of aerial vehicles inspired by coordinated behaviors of such biological groups. The following key points will be taken into account. First, the model will be based on a sequence of simple rules followed by every individual (microscopic level). Then, it will include constraints related to limited sensor information. Moreover, since many applications occur in a high density traffic environment, the model will result in safe paths for all individuals.

To reach our objective, we consider an interacting particle system for the collective behavior of swarms [6, 7]. In behavioral based methods, all the agents are considered equal and they adopt behaviors built on informations coming from their only neighborhood. Thanks to the feedback shared between neighboring agents, these methods are following a decentralized approach. In high density traffic situations, it is recommended to use a decentralized coordination [22], even if there is less freedom for maneuver. However, it is usually difficult to predict the group behavior, and the stability of the formation is generally not easy to prove either. These methods are among the first to have been used in motion planning for multi-agent systems as they are easily stated and generally efficiently scalable since their rules are supposed to be implemented independently for each agent.

Safe paths is related to collision avoidance which plays an important role in the context of managing multiple vehicles. It has been an active area of research in the field of robotics using the collision cone method [8] and the inevitable collision states approach [17, 21]. The collision cone approach can be used to determine whether two objects, of irregular shapes and arbitrary sizes, are on a collision course. It has been the basis for many collision/obstacle avoidance algorithms [8]. These methods are developed with robotic application with knowledge about the obstacles (position, velocity, and acceleration) [21]. There have been also some research on aircraft collision avoidance both from the multiple vehicles and the air traffic control points of view. All these collision avoidance procedures are based on three steps : see, detect, and avoid [26]. But most of the algorithms developed for air traffic management are those that guarantee safe trajectories in a very low density traffic involving only two or three aircraft. Another approach for collision avoidance is artificial potential based methods where individuals are treated like charged particles of same charge that repel each other; whereas the destination of an individual is modeled as a charge of the opposite sign so as to attract or navigate it toward the destination. The artificial potential methods are susceptible to local minima and require breaking forces [12, 13].

In this paper, our goal is first to develop a three dimensional dynamical approach describing the motions of N individual and interacting particles, when N becomes large. The model is inspired from the ones developed in [9, 10] and [14, 15] for pedestrians collective motion in 2D but here we are concerned with 3D motion of aerial vehicles or birds which leads to an enhanced but more complex dynamics. Based on the vision based approach, we propose a model decomposed in two phases for collision avoidance including both particle to particle and moving obstacles avoidance.

When dealing with large populations, in both cases one faces the well-known problem of the curse of dimensionality, term first coined by Bellman precisely in the context of dynamic optimization: the complexity of numerical computations of the solutions of the above problems blows up as the size of

the population increases. A possible way out is the so-called mean-field approach, where the individual influence of the entire population on the dynamics of a single agent is replaced by an averaged one. This substitution principle results in a unique mean-field equation and allows the computation of solutions, cutting loose from the dimensionality. Therefore, we perform a mean field limit of the microscopic model to replace self-interactions between particles by self-consistent fields. The mean field approximation corresponds to the case where the force itself depends on some average of the distribution function. As a consequence, binary interactions between particles are not described but instead their global effect on each particle is taken into account. This approximation is justified especially in the configuration where the swarm is very closed to the target and therefore identifying binary interaction is very complex. As a result, we obtain a space-inhomogeneous kinetic PDE.

The remainder of the paper is organized as follows. In Section 2, we present the individual agent based model proposed for self-propelled particle swarms including collision avoidance. In Section 3, the associated mean-field limit is formally derived and analysed. Section 4 is devoted to numerical experiments of the microscopic model. We conclude with final remarks and future works in Section 5.

2. AGENT-BASED MODEL FOR COLLISION AVOIDANCE

We are interested in modeling the motion of individuals (vehicles, birds,..) with the objective to drive each individual of the swarm to a target point \mathbf{x}_T without colliding with any moving obstacles or other individuals.

Since we consider a swarm we do not explicitly constrain the relative location of each individual. This section is devoted to the presentation of the microscopic model considering N particles with position $\mathbf{x}_i(t) \in \mathbb{R}^3$ and velocity $\mathbf{v}_i(t) \in \mathbb{R}^3$, with $1 \leq i \leq N$. Then, we derive a three-dimensional interacting particle system based on collision avoidance. The agent-based model we consider is inspired from the one proposed in [9],[10] and [28] developed for crowd dynamics. In these references, the heuristic-based model proposes that pedestrians follow a rule composed of two phases:

- (1) a perception phase;
- (2) a decision-making phase.

In the perception phase, the subjects make an assessment of the dangerousness of the possible encounters in all the possible directions of motion. In the decision-making phase, they turn towards the direction which minimizes the distance walked towards their target while avoiding encounters with other pedestrians. Here, we mainly follow the same assumptions to describe the perception phase, but then the individual changes its direction in order to diminish the probability of collision.

As we will describe later particles may accelerate or break smoothly according to their distance to the target, but during the collision avoidance process, a sudden change of speed in the air is not realistic, hence particles will only change their own direction. Therefore, in the perception and decision making phases, we assume that particles move with a constant speed, which means that interacting particles cannot evaluate the change of speed of each other. Of course in some situations, avoidance may fail when the relative distance is too small or the relative velocity is too large or when particles are not fast enough to change their direction. This corresponds to physical situations where a crash cannot be systematically avoided.

2.1. Perception Phase. We consider a particle $i \in \{1, \dots, N\}$ located at a position $\mathbf{x}_i(t) \in \mathbb{R}^3$, with a velocity $\mathbf{v}_i(t)$, interacting with a collision partner $j \in \{1, \dots, N\}$ located at a position $\mathbf{x}_j(t) \in \mathbb{R}^3$, with a velocity $\mathbf{v}_j(t)$. The sketch of the binary encounter between these two particles is depicted in Figure 1. In the sequel we denote by $\langle \cdot, \cdot \rangle$ the usual scalar product in \mathbb{R}^3 ,

$$\langle \mathbf{u}, \mathbf{v} \rangle = \sum_{i=1}^3 u_i v_i$$

and by $|\mathbf{u}| = \sqrt{\langle \mathbf{u}, \mathbf{u} \rangle}$ the associated norm.

We assume that $t = t^0$ is the time when particle i evaluates the likeliness of a collision with particle j . This evaluation is made by supposing that each one maintains its velocity \mathbf{v}_i , (respectively \mathbf{v}_j)

constant. As depicted in Figure 1, we introduce two notable points $\bar{\mathbf{x}}_i$ and $\bar{\mathbf{x}}_j$ that we define just below.

Definition 2.1. *The interaction points $\bar{\mathbf{x}}_i$ (resp. $\bar{\mathbf{x}}_j$) of particle i (resp. j) in their interaction is the point $\mathbf{x}_i(t)$ on the i -th particle's trajectory (resp. $\mathbf{x}_j(t)$ on the j -th particle's trajectory) such that $|\mathbf{x}_i(t) - \mathbf{x}_j(t)|$ is minimal, i.e.*

$$|\bar{\mathbf{x}}_i - \bar{\mathbf{x}}_j| = \min_{t \in \mathbb{R}} |\mathbf{x}_i(t) - \mathbf{x}_j(t)|.$$

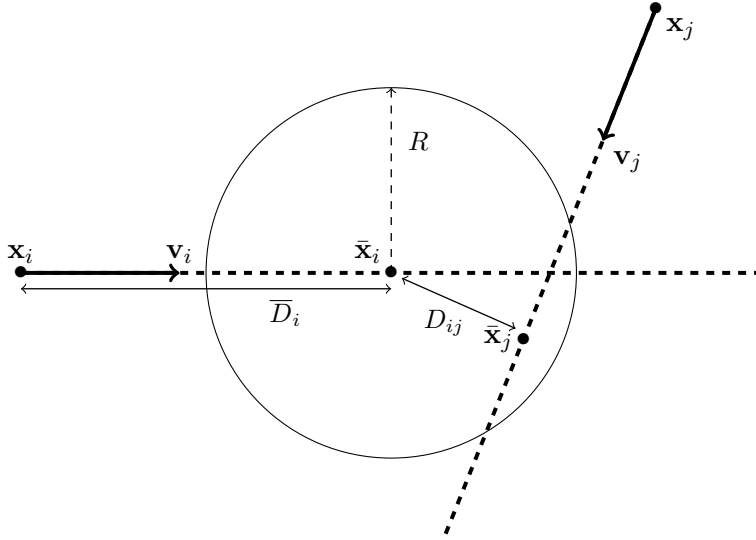


FIGURE 1. Sketch of a binary encounter between two particles in 2D showing the key distances of the perception phase: the Minimal Distance D_{ij} (distance between $\bar{\mathbf{x}}_i$ and $\bar{\mathbf{x}}_j$) and the Distance-To-Interaction \bar{D}_i of particle i in its interaction with particle j (distance between the current particle position \mathbf{x}_i and $\bar{\mathbf{x}}_i$). The circle with radius R delimits the safety region for the particle i .

Definition 2.2. *The interaction between particles i and j leads to define three key quantities associated to perception phase:*

- *The minimal distance D_{ij} represents the smallest distance which separates the two particles i and j supposing that they cruise on a straight line at constant velocities \mathbf{v}_i and \mathbf{v}_j . From Definition 2.1, the minimal distance is then the distance between the interaction points such that*

$$D_{ij} = |\bar{\mathbf{x}}_i - \bar{\mathbf{x}}_j|.$$

- *The time-to-interaction τ_{ij} is the time needed by the subject to reach the interaction point $\bar{\mathbf{x}}_i$ from his current position $\mathbf{x}_i = \mathbf{x}_i(t^0)$ at time t^0 , which is counted positive if this time belongs to the future of the subject and negative if it belongs to the past. Then, τ_{ij} is the value of t for which the quantity $|\mathbf{x}_i(t) - \mathbf{x}_j(t)|$ is minimal.*
- *The distance-to-interaction \bar{D}_i is the distance which separates the subject's current position $\mathbf{x}_i = \mathbf{x}_i(t^0)$ to the interaction point $\bar{\mathbf{x}}_i$. The distance-to-interaction is counted positive if the interaction point is reached in the future and negative if the interaction point was crossed in the past:*

$$\bar{D}_i = \text{sign}(t - t^0) |\mathbf{x}_i - \bar{\mathbf{x}}_i|,$$

where $\text{sign}(t)$ denotes the sign of t .

Remark 2.3. *Notice that the quantities D_{ij} and τ_{ij} are symmetric with respect to i and j . Moreover, here, we have supposed that each individual has a perfect knowledge of its own and partners positions and velocities, and we assume that they are able to estimate or to compute the distance-to-interaction,*

the minimal distance and the time to interaction with perfect accuracy from the knowledge of $(\mathbf{x}_i, \mathbf{v}_i)$ and $(\mathbf{x}_j, \mathbf{v}_j)$.

Let us now compute τ_{ij} , \bar{D}_i and D_{ij} assuming that a particle i with a phase space position $(\mathbf{x}_i, \mathbf{v}_i)$ can detect an interaction's partner j located in its perception region with a position \mathbf{x}_j and velocity \mathbf{v}_j . We follow the same strategy as for two dimensional pedestrian flow [9] and denoting by \mathbf{x}_i and \mathbf{x}_j the positions of the two particles at time t^0 , we define the distance $D(t)$ between the two particles at time $t \in (t^0, t^0 + \delta t)$ by

$$(2.1) \quad D^2(t) = |\mathbf{x}_j + \mathbf{v}_j(t - t^0) - (\mathbf{x}_i + \mathbf{v}_i(t - t^0))|^2$$

Therefore, for each particle i and its interaction partner j , we have the following result.

Proposition 2.4. *The value of the time to interaction for the particle i , τ_{ij} is*

$$(2.2) \quad \tau_{ij} = -\frac{\langle \mathbf{x}_j - \mathbf{x}_i, \mathbf{v}_j - \mathbf{v}_i \rangle}{|\mathbf{v}_j - \mathbf{v}_i|^2},$$

whereas the distance to interaction \bar{D}_i of particle i and the minimal distance D_{ij} are given by

$$(2.3) \quad \bar{D}_i = -\frac{\langle \mathbf{x}_j - \mathbf{x}_i, \mathbf{v}_j - \mathbf{v}_i \rangle}{|\mathbf{v}_j - \mathbf{v}_i|^2} |\mathbf{v}_i|$$

and

$$(2.4) \quad D_{ij} = \left(|\mathbf{x}_j - \mathbf{x}_i|^2 - \left(\frac{\langle \mathbf{x}_j - \mathbf{x}_i, \mathbf{v}_j - \mathbf{v}_i \rangle}{|\mathbf{v}_j - \mathbf{v}_i|} \right)^2 \right)^{1/2}.$$

Proof. On the one hand, the value of the time to interaction for the particle i , is obtained by minimizing the quadratic function of time (2.1) such that

$$D^2(t) = |\mathbf{v}_j - \mathbf{v}_i|^2 \left((t - t^0) + \frac{\langle \mathbf{x}_j - \mathbf{x}_i, \mathbf{v}_j - \mathbf{v}_i \rangle}{|\mathbf{v}_j - \mathbf{v}_i|^2} \right)^2 + |\mathbf{x}_j - \mathbf{x}_i|^2 - \frac{\langle \mathbf{x}_j - \mathbf{x}_i, \mathbf{v}_j - \mathbf{v}_i \rangle^2}{|\mathbf{v}_j - \mathbf{v}_i|^2},$$

hence it gives $\tau_{i,j}$ as in (2.2). Then, the distance to interaction \bar{D}_i of particle i is given by the distance traveled by this particle during the time to interaction, that is, $\bar{D}_i = \tau_{ij} |\mathbf{v}_i|$ where τ_{ij} is given by Definition 2.2. This leads to \bar{D}_i as in (2.3).

On the other hand, the minimal distance D_{ij} is given by the minimal value of (2.1), it gives $D_{ij} = D(t^0 + \tau_{ij})$, which leads to (2.4). \square

The objective of the perception phase is to describe the configuration corresponding to a potential collision of the particle i with the surrounding particles. From the definitions of the minimal distance and time-to-interaction, we consider that a collision may occur between particle i and particle j when the following conditions are satisfied.

- First, we need $\tau_{ij} > 0$ that means that we observe in the future.
- Second, if we define a safety zone for the particle i delimited by the circle of radius R as depicted in Figure 1 then collision will occur if $D_{ij} \leq R$.

Combining these two conditions mean that in the future, the trajectories of each particle will encounter inside the safety zone. Therefore, we define the set of particles which may interact with a particle i located at $(\mathbf{x}_i, \mathbf{v}_i) \in \mathbb{R}^3 \times \mathbb{R}^3$ at time t^0 , as

$$\mathcal{I}_i(t^0) = \left\{ j \in \{0, \dots, N\}, \tau_{ij} > 0, D_{ij} \leq R \right\}.$$

However, some restrictions related to the perception sensitivity of the individual (vision, sensors, etc) has also to be taken into account. As a consequence, considering a test particle i interacting with another particle $j \in \mathcal{I}_i(t^0)$, we restrict the set of potential partner collision to those belonging to the ‘‘vision cone’’ of particle i denoted \mathcal{C}_i . This region is represented for instance as the blue area in Figure 2 and model the set of positions for the particle $j \in \mathcal{I}_i(t^0)$ that are seen by the particle i . Let us now define the ‘‘vision cone’’ \mathcal{C}_i precisely.

Definition 2.5 (Vision cone). *Introducing a threshold number $\kappa \in [-1, 1]$, the “vision cone” \mathcal{C}_i for the particle i is the cone centered at \mathbf{x}_i with angle $\cos^{-1}(\kappa)$ about the direction \mathbf{v}_i .*

Remark 2.6. *Observe that in Definition 2.5, we choose the vision cone such that it has an infinite radius, but the relative distance and velocity between two particles will be taken into account thanks to the parameter $\tau_{ij} > 0$, where the collision avoidance’s frequency will be a decreasing function of τ_{ij} . However, the present model can be adapted without any difficulty to the case where the vision cone is also limited by its distance.*

To summarize the perception phase, for each particle i we define the set of interaction’s partners as the set

$$(2.5) \quad \mathcal{K}_i(t^0) = \{j \in \mathcal{I}_i(t^0), \mathbf{x}_j \in \mathcal{C}_i\}.$$

So we now detail the Decision Making Phase in order to model collision avoidance.

2.2. Decision Making Phase. First let us emphasize that the three dimensional swarm modeling is quite different from the two dimensional case encountered in collision avoidance for pedestrians or robots [28]. Indeed, in the three dimensional case, particles cannot suddenly stop or brake!

Here we consider the motion of a particle $i \in \{1, \dots, N\}$ with position and velocity $(\mathbf{x}_i, \mathbf{v}_i) \in \mathbb{R}^3 \times \mathbb{R}^3$, which interacts with a particle $j \in \{1, \dots, N\}$ located at $(\mathbf{x}_j, \mathbf{v}_j) \in \mathbb{R}^3 \times \mathbb{R}^3$. Depending on the position of the interaction points $(\bar{\mathbf{x}}_i, \bar{\mathbf{x}}_j) \in \mathbb{R}^3 \times \mathbb{R}^3$, the collision avoidance procedure leads to consider three configurations:

- Safe configuration (illustrated in Figure 2-(a)), where the particle i does not change its direction and continues its cruise;
- Blind configuration (illustrated in Figure 2-(b)), where a collision is likely, but particle i does not see j , hence it continues its cruise whereas j is expected to modify its direction;
- Unsafe configuration (illustrated on Figure 2-(c)), where the particle i has detected an interaction’s partner j and both of them modify their direction.

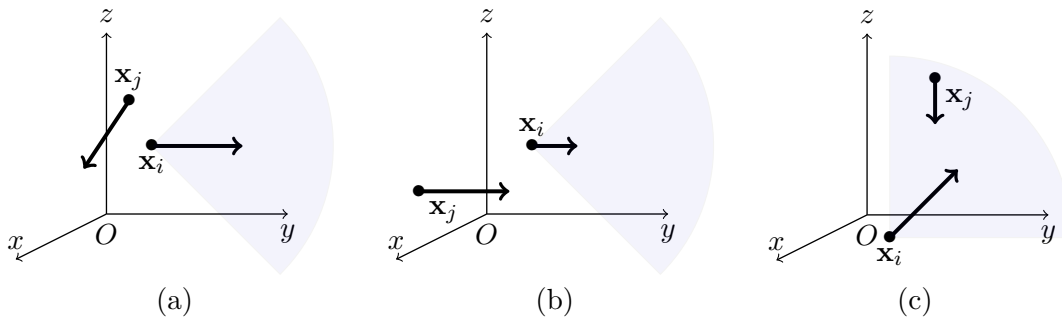


FIGURE 2. Depending on the cone definition of the particle i , several configurations occur: (a) safe configuration where the two particles do not interact (b) blind configuration where i does not interact with j , but j is expected to change its direction (c) unsafe configuration where both particles will change their direction.

To describe more precisely this turning process, we introduce the local frame of the particle $i \in \{1, \dots, N\}$ centered at position $\mathbf{x}_i(t) \in \mathbb{R}^3$, and denoted by $(\mathbf{e}_{\rho_i}, \mathbf{e}_{\phi_i}, \mathbf{e}_{\theta_i})$ with $\rho_i(t) = |\mathbf{v}_i(t)|$, $\theta_i \in (0, 2\pi)$ the azimuthal angle and $\phi_i \in (0, \pi)$ the polar angle giving that $\mathbf{v}_i = \rho_i \mathbf{e}_{\rho_i}$.

The collision avoidance model proposed below is based on the situation where a particle $i \in \{1, \dots, N\}$ interacts with another one $j \in \mathcal{K}_i(t^0)$ and will modify its direction but preserve its speed, that is, $\rho_i(t)$ is maintained constant during this process. To determine this turning rate and the rotation axis, we need to define some indicators on occurrence of collisions. The first indicator of the dangerousness of the collision is the time τ_{ij} , which indicates the remaining time before a collision occurs. The second indicator measured by particle i , is the time derivative of the relative bearing

angle or azimuthal angle $\alpha_{ij} \in (0, 2\pi)$ and the relative polar angle $\beta_{ij} \in (0, \pi)$ formed in its own frame between the direction \mathbf{v}_i and the position \mathbf{x}_j of particle $j \in \mathcal{K}(t^0)$ as depicted in Figure 3.

To define rigorously these two angles and their time derivative we need to consider the frame $(\mathbf{e}_{\rho_i}, \mathbf{e}_{\phi_i}, \mathbf{e}_{\theta_i})$ of the particle i at position $\mathbf{x}_i \in \mathbb{R}^3$ with velocity $\mathbf{v}_i \in \mathbb{R}^3$.

Definition 2.7 (relative azimuthal and polar angles). *Consider the local frame $(\mathbf{e}_{\rho_i}, \mathbf{e}_{\phi_i}, \mathbf{e}_{\theta_i})$ centered in at \mathbf{x}_i of the particle $i \in \{1, \dots, N\}$, and denote by $j \in \mathcal{K}_i(t^0)$ its collision partner located at $(\mathbf{x}_j, \mathbf{v}_j) \in \mathbb{R}^6$. We define*

- the relative bearing or azimuthal angle $\alpha_{ij} \in (0, 2\pi)$ as the azimuthal angle of point \mathbf{x}_j with respect to the plane containing the point \mathbf{x}_i and formed by the two vectors $(\mathbf{e}_{\rho_i}, \mathbf{e}_{\phi_i})$;
- the relative polar angle $\beta_{ij} \in (0, \pi)$ as the polar angle of point \mathbf{x}_j with respect to the vector \mathbf{e}_{θ_i} .

The choice of α_{ij} and β_{ij} is here somehow arbitrary as long as we obtain an orthonormal basis as we will see below.

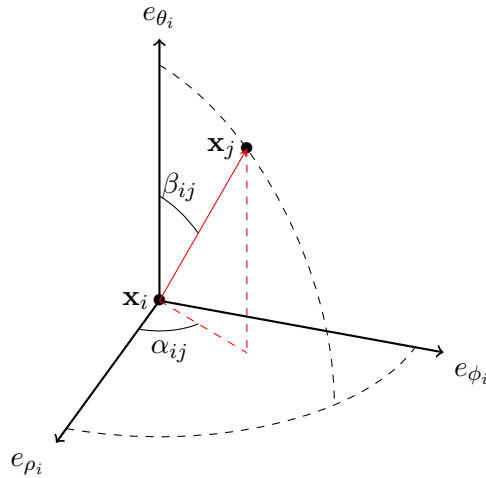


FIGURE 3. Definition of the relative bearing angle $\alpha_{ij} \in (0, 2\pi)$ as the azimuthal angle of point \mathbf{x}_j in the frame $(\mathbf{e}_{\rho_i}, \mathbf{e}_{\phi_i}, \mathbf{e}_{\theta_i})$ centered at \mathbf{x}_i and of the relative polar angle $\beta_{ij} \in (0, \pi)$ as the polar angle of point \mathbf{x}_j in the frame $(\mathbf{e}_{\rho_i}, \mathbf{e}_{\phi_i}, \mathbf{e}_{\theta_i})$ centered at \mathbf{x}_i .

We also introduce the unit vector \mathbf{k}_{ij} of the line connecting the two particles and the distance d_{ij} between the particles. These quantities are defined by the following relations:

$$(2.6) \quad \begin{cases} d_{ij}(t) = |\mathbf{x}_j(t) - \mathbf{x}_i(t)|, \\ \mathbf{k}_{ij}(t) = \frac{\mathbf{x}_j(t) - \mathbf{x}_i(t)}{d_{ij}(t)}. \end{cases}$$

Then we perform a new change of frame with respect to $\mathbf{x}_i - \mathbf{x}_j$, and introduce the orthonormal frame defined as $(\mathbf{k}_{ij}, \mathbf{e}_{\beta_{ij}}, \mathbf{e}_{\alpha_{ij}})$, where

$$(2.7) \quad \begin{cases} \mathbf{e}_{\beta_{ij}} = \cos(\beta_{ij}) \cos(\alpha_{ij}) \mathbf{e}_{\rho_i} + \cos(\beta_{ij}) \sin(\alpha_{ij}) \mathbf{e}_{\phi_i} - \sin(\beta_{ij}) \mathbf{e}_{\theta_i}, \\ \mathbf{e}_{\alpha_{ij}} = -\sin(\alpha_{ij}) \mathbf{e}_{\rho_i} + \cos(\alpha_{ij}) \mathbf{e}_{\phi_i}. \end{cases}$$

Notice that in three dimensions, there are several possibilities to define relative azimuthal and polar angles, but this choice is arbitrary as long as we obtain an orthonormal basis. Then we compute the time derivative of α_{ij} and β_{ij} which will be a key indicator in the collision avoidance process.

Lemma 2.8. *Assume that particles (i, j) are at time t^0 at positions \mathbf{x}_i and \mathbf{x}_j , and move with constant velocity \mathbf{v}_i and \mathbf{v}_j . Then*

$$(2.8) \quad \dot{\beta}_{ij} = \frac{1}{d_{ij}} \langle \mathbf{v}_j - \mathbf{v}_i, \mathbf{e}_{\beta_{ij}} \rangle, \quad \sin(\beta_{ij}) \dot{\alpha}_{ij} = \frac{1}{d_{ij}} \langle \mathbf{v}_j - \mathbf{v}_i, \mathbf{e}_{\alpha_{ij}} \rangle,$$

Proof. By the definition of the relative bearing angle $\alpha_{ij} \in (0, 2\pi)$ and the relative polar angle $\beta_{ij} \in (0, \pi)$, we can write:

$$\mathbf{k}_{ij} = \sin(\beta_{ij}) \cos(\alpha_{ij}) \mathbf{e}_{\rho_i} + \sin(\beta_{ij}) \sin(\alpha_{ij}) \mathbf{e}_{\phi_i} + \cos(\beta_{ij}) \mathbf{e}_{\theta_i}.$$

Taking the time derivative of this relation and using the fact that $(\mathbf{e}_{\rho_i}, \mathbf{e}_{\theta_i}, \mathbf{e}_{\phi_i})$ is constant since the motion of the particle i is supposed rectilinear with constant speed \mathbf{v}_i , it leads to

$$\begin{aligned} \dot{\mathbf{k}}_{ij} &= \dot{\beta}_{ij} [\cos(\beta_{ij}) \cos(\alpha_{ij}) \mathbf{e}_{\rho_i} + \cos(\beta_{ij}) \sin(\alpha_{ij}) \mathbf{e}_{\phi_i} - \sin(\beta_{ij}) \mathbf{e}_{\theta_i}] \\ &\quad + \sin(\beta_{ij}) \dot{\alpha}_{ij} [-\sin(\alpha_{ij}) \mathbf{e}_{\rho_i} + \cos(\alpha_{ij}) \mathbf{e}_{\phi_i}], \end{aligned}$$

where we recognize the expression of the two unit vectors $(\mathbf{e}_{\alpha_{ij}}, \mathbf{e}_{\beta_{ij}})$ constructed in (2.7) by writing the point \mathbf{x}_j in spherical coordinates in the frame of particle i . Hence we have

$$(2.9) \quad \dot{\mathbf{k}}_{ij} = \dot{\beta}_{ij} \mathbf{e}_{\beta_{ij}} + \sin(\beta_{ij}) \dot{\alpha}_{ij} \mathbf{e}_{\alpha_{ij}}.$$

On the other hand, observing that

$$d_{ij} = \langle \mathbf{v}_j - \mathbf{v}_i, \mathbf{k}_{ij} \rangle$$

and taking the time derivative of the first equation (2.6), it yields

$$\begin{aligned} \dot{\mathbf{k}}_{ij} &= \frac{d}{dt} \left(\frac{\mathbf{x}_j - \mathbf{x}_i}{d_{ij}} \right), \\ &= \frac{1}{d_{ij}} [(\mathbf{v}_j - \mathbf{v}_i) - \langle \mathbf{v}_j - \mathbf{v}_i, \mathbf{k}_{ij} \rangle \mathbf{k}_{ij}], \end{aligned}$$

hence using the fact that $(\mathbf{k}_{ij}, \mathbf{e}_{\alpha_{ij}}, \mathbf{e}_{\beta_{ij}})$ constitutes an orthonormal basis, we finally have

$$(2.10) \quad \dot{\mathbf{k}}_{ij} = \frac{1}{d_{ij}} [\langle \mathbf{v}_j - \mathbf{v}_i, \mathbf{e}_{\alpha_{ij}} \rangle \mathbf{e}_{\alpha_{ij}} + \langle \mathbf{v}_j - \mathbf{v}_i, \mathbf{e}_{\beta_{ij}} \rangle \mathbf{e}_{\beta_{ij}}].$$

Identifying the two relations (2.9) and (2.10), we get $\dot{\beta}_{ij}$ and $\sin(\beta_{ij}) \dot{\alpha}_{ij}$, which gives rise to formula (2.8) for the derivative of the relative bearing and polar angles. \square

We are now ready to make the link between the time derivative of the relative polar and bearing angles and the collision avoidance process. Assume that $t = t^0$ and consider two particles $(i, j) \in \{1, \dots, N\}^2$, such that $j \in \mathcal{I}_i(t^0)$. In the present situation the two interaction points $\bar{\mathbf{x}}_i$ and $\bar{\mathbf{x}}_j$ are relatively close and the particles need to rotate to avoid a collision, so that, the minimal distance D_{ij} , given in (2.4), will increase. Then, we write $\mathbf{v}_j - \mathbf{v}_i$ in the orthonormal frame $\{\mathbf{k}_{ij}, \mathbf{e}_{\beta_{ij}}, \mathbf{e}_{\alpha_{ij}}\}$ and using the results of Lemma 2.8, it yields that

$$|\mathbf{v}_j - \mathbf{v}_i|^2 = d_{ij}^2 \left(|\dot{\beta}_{ij}|^2 + |\sin(\beta_{ij}) \dot{\alpha}_{ij}|^2 \right) + \langle \mathbf{v}_j - \mathbf{v}_i, \mathbf{k}_{ij} \rangle^2,$$

hence we have

$$\begin{aligned} D_{ij}^2 &= \left(\frac{d_{ij}}{|\mathbf{v}_j - \mathbf{v}_i|} \right)^2 (|\mathbf{v}_j - \mathbf{v}_i|^2 - \langle \mathbf{v}_j - \mathbf{v}_i, \mathbf{k}_{ij} \rangle^2), \\ &= \left(\frac{d_{ij}^2}{|\mathbf{v}_j - \mathbf{v}_i|} \right)^2 \mathcal{A}_{ij}^2, \end{aligned}$$

where \mathcal{A}_{ij}^2 is defined as

$$(2.11) \quad \mathcal{A}_{ij}^2(t) := \dot{\beta}_{ij}^2(t) + |\sin(\beta_{ij}) \dot{\alpha}_{ij}(t)|^2.$$

This results indicates that the collision is very likely when $\mathcal{A}_{ij}^2(t^0)$ is small. Therefore, to increase the minimal distance D_{ij} we need to increase the magnitude of the time derivative of the relative

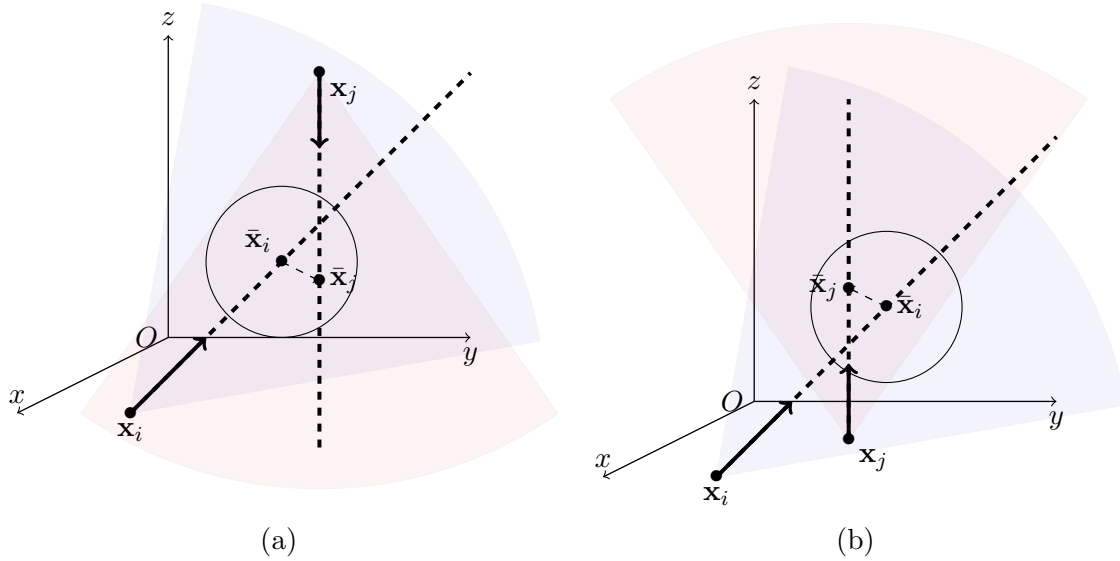


FIGURE 4. Vision cones for each particle (\mathcal{C}_i in blue and \mathcal{C}_j in pink) for the two considered configurations: (a) cooperative interactions, (b) non cooperative interactions

bearing and polar angle $(\sin(\beta_{ij}) \dot{\alpha}_{ij}, \dot{\beta}_{ij})$ given in Lemma 2.8. Thus, the proposed control scheme is based on gyroscopic forces but adapted to the constraints due to the perception region. On the one hand we consider the situation where the two particles see each other, then they cooperate to avoid collisions (cooperative interaction represented in Figure 4-(a)). On the other hand, we describe the interaction of one particle with an obstacle or another particle which do not deviate from its trajectory (non-cooperative interaction represented in Figure 4-(b)).

2.2.1. Cooperative interactions. At time $t = t^0$, both particles are such that $(i, j) \in \mathcal{K}_j(t^0) \times \mathcal{K}_i(t^0)$ as it is shown in Figure 4-(a). Then the two particles will rotate in order to avoid to collide along a rotation axis defined by a vector field \mathbf{R}_{ij} which has to be determined such that

$$\begin{cases} \frac{d\mathbf{v}_i}{dt} = \omega_{ij} \mathbf{v}_i \wedge \mathbf{R}_{ij}, \\ \frac{d\mathbf{v}_j}{dt} = \omega_{ij} \mathbf{v}_j \wedge \mathbf{R}_{ij}, \end{cases}$$

where $\omega_{ij} > 0$ defines the rotation frequency. To this aim, we write the vector \mathbf{R}_{ij} in the basis $\{\mathbf{k}_{ij}, \mathbf{e}_{\beta_{ij}}, \mathbf{e}_{\alpha_{ij}}\}$ as

$$(2.12) \quad \mathbf{R}_{ij} = r_{ij}^1 \mathbf{k}_{ij} + r_{ij}^2 \mathbf{e}_{\beta_{ij}} + r_{ij}^3 \mathbf{e}_{\alpha_{ij}}$$

and determine the values of $(r_{ij}^1, r_{ij}^2, r_{ij}^3)$ in order to increase the magnitude of $(\sin(\beta_{ij}) \dot{\alpha}_{ij}, \dot{\beta}_{ij})$. In the next lemma, we determine the rotation axis and show how to increase the time derivative of the bearing and polar angles and therefore, thus decreasing the likeliness of the collision. We follow the same strategy as [10] for two dimensional problems.

Lemma 2.9. *Assume that two particles $(i, j) \in \{1, \dots, N\}^2$ are such that $(i, j) \in \mathcal{K}_j(t^0) \times \mathcal{K}_i(t^0)$ and consider the time derivative of the relative bearing and polar angles $(\sin(\beta_{ij}) \dot{\alpha}_{ij}, \dot{\beta}_{ij})$ given in (2.8) and the rotational axis \mathbf{R}_{ij} given by (2.12) is such that $r_{ij}^1 \in \mathbb{R}$,*

$$(2.13) \quad -\frac{\omega_{ij} r_{ij}^3}{\dot{\beta}_{ij}} \leq 2 \quad \text{and} \quad \frac{\omega_{ij} r_{ij}^2}{\sin(\beta_{ij}) \dot{\alpha}_{ij}} \leq 2.$$

Then, $(\sin(\beta_{ij}) \dot{\alpha}_{ij}, \dot{\beta}_{ij})$ is solution to the following system

$$(2.14) \quad \begin{cases} \frac{d\dot{\beta}_{ij}}{dt} = (\omega_{ij} r_{ij}^1 + \cos(\beta_{ij}) \dot{\alpha}_{ij}) \sin(\beta_{ij}) \dot{\alpha}_{ij} + \lambda_{ij}^3 \dot{\beta}_{ij}, \\ \frac{d}{dt} (\sin(\beta_{ij}) \dot{\alpha}_{ij}) = -(\omega_{ij} r_{ij}^1 + \cos(\beta_{ij}) \dot{\alpha}_{ij}) \dot{\beta}_{ij} + \lambda_{ij}^2 \sin(\beta_{ij}) \dot{\alpha}_{ij}, \end{cases}$$

with

$$(2.15) \quad \begin{cases} \lambda_{ij}^3 := \left(2 + \frac{\omega_{ij} r_{ij}^3}{\dot{\beta}_{ij}}\right) \left(\frac{|\mathbf{v}_j - \mathbf{v}_i|}{d_{ij}}\right)^2 \tau_{ij} \in \mathbb{R}^+, \\ \lambda_{ij}^2 := \left(2 - \frac{\omega_{ij} r_{ij}^2}{\sin(\beta_{ij}) \dot{\alpha}_{ij}}\right) \left(\frac{|\mathbf{v}_j - \mathbf{v}_i|}{d_{ij}}\right)^2 \tau_{ij} \in \mathbb{R}^+. \end{cases}$$

Furthermore, \mathcal{A}_{ij}^2 given in (2.11) satisfies for $\gamma_{ij} = \min(\lambda_{ij}^2, \lambda_{ij}^3)$,

$$(2.16) \quad \frac{d\mathcal{A}_{ij}^2}{dt} \geq \frac{\gamma_{ij}}{2} \mathcal{A}_{ij}^2.$$

Proof. Let us consider the expression of $(\sin(\beta_{ij}) \dot{\alpha}_{ij}, \dot{\beta}_{ij})$ given by (2.8). Then we compute the time derivative of both quantities

$$\begin{aligned} \frac{d\dot{\beta}_{ij}}{dt} &= \frac{1}{d_{ij}} (\langle \dot{\mathbf{v}}_j - \dot{\mathbf{v}}_i, \mathbf{e}_{\beta_{ij}} \rangle + \langle \mathbf{v}_j - \mathbf{v}_i, \dot{\mathbf{e}}_{\beta_{ij}} \rangle) \\ &\quad - \frac{1}{d_{ij}^3} \langle \mathbf{v}_j - \mathbf{v}_i, \mathbf{x}_j - \mathbf{x}_i \rangle \langle \mathbf{v}_j - \mathbf{v}_i, \mathbf{e}_{\beta_{ij}} \rangle \end{aligned}$$

and

$$\begin{aligned} \frac{d}{dt} (\sin(\beta_{ij}) \dot{\alpha}_{ij}) &= \frac{1}{d_{ij}} (\langle \dot{\mathbf{v}}_j - \dot{\mathbf{v}}_i, \mathbf{e}_{\alpha_{ij}} \rangle + \langle \mathbf{v}_j - \mathbf{v}_i, \dot{\mathbf{e}}_{\alpha_{ij}} \rangle) \\ &\quad - \frac{1}{d_{ij}^3} \langle \mathbf{v}_j - \mathbf{v}_i, \mathbf{x}_j - \mathbf{x}_i \rangle \langle \mathbf{v}_j - \mathbf{v}_i, \mathbf{e}_{\alpha_{ij}} \rangle. \end{aligned}$$

Now we observe that

$$\begin{cases} \dot{\mathbf{e}}_{\alpha_{ij}} = -\dot{\alpha}_{ij} [\cos(\beta_{ij}) \mathbf{e}_{\beta_{ij}} + \sin(\beta_{ij}) \mathbf{k}_{ij}], \\ \dot{\mathbf{e}}_{\beta_{ij}} = +\dot{\alpha}_{ij} \cos(\beta_{ij}) \mathbf{e}_{\alpha_{ij}} - \dot{\beta}_{ij} \mathbf{k}_{ij}, \end{cases}$$

hence using the definition of the unit vector \mathbf{k}_{ij} in (2.6) and the definition of τ_{ij} in (2.2), it yields for the time derivative of the relative polar angle β_{ij} ,

$$\frac{d\dot{\beta}_{ij}}{dt} = \omega_{ij} \frac{\langle (\mathbf{v}_j - \mathbf{v}_i) \wedge \mathbf{R}_{ij}, \mathbf{e}_{\beta_{ij}} \rangle}{d_{ij}} + \cos(\beta_{ij}) \sin(\beta_{ij}) \dot{\alpha}_{ij}^2 + 2 \left(\frac{|\mathbf{v}_j - \mathbf{v}_i|}{d_{ij}}\right)^2 \tau_{ij} \dot{\beta}_{ij},$$

then for the time derivative of $\sin(\beta_{ij}) \dot{\alpha}_{ij}$,

$$\frac{d}{dt} (\sin(\beta_{ij}) \dot{\alpha}_{ij}) = \omega_{ij} \frac{\langle (\mathbf{v}_j - \mathbf{v}_i) \wedge \mathbf{R}_{ij}, \mathbf{e}_{\alpha_{ij}} \rangle}{|\mathbf{x}_j - \mathbf{x}_i|} - \cos(\beta_{ij}) \dot{\beta}_{ij} \dot{\alpha}_{ij} + 2 \left(\frac{|\mathbf{v}_j - \mathbf{v}_i|}{|\mathbf{x}_j - \mathbf{x}_i|}\right)^2 \tau_{ij} \sin(\beta_{ij}) \dot{\alpha}_{ij}.$$

Therefore, from the definition of \mathbf{R}_{ij} in (2.12) and using that $\langle \mathbf{a}, \mathbf{b} \wedge \mathbf{c} \rangle = \langle \mathbf{b}, \mathbf{c} \wedge \mathbf{a} \rangle$, we get

$$\begin{cases} \langle (\mathbf{v}_j - \mathbf{v}_i) \wedge \mathbf{R}_{ij}, \mathbf{e}_{\beta_{ij}} \rangle = +r_{ij}^1 \langle \mathbf{v}_j - \mathbf{v}_i, \mathbf{e}_{\alpha_{ij}} \rangle - r_{ij}^3 \langle \mathbf{v}_j - \mathbf{v}_i, \mathbf{k}_{ij} \rangle, \\ \langle (\mathbf{v}_j - \mathbf{v}_i) \wedge \mathbf{R}_{ij}, \mathbf{e}_{\alpha_{ij}} \rangle = -r_{ij}^1 \langle \mathbf{v}_j - \mathbf{v}_i, \mathbf{e}_{\beta_{ij}} \rangle + r_{ij}^2 \langle \mathbf{v}_j - \mathbf{v}_i, \mathbf{k}_{ij} \rangle, \end{cases}$$

which gives using (2.8), the system of equations given in (2.14) with (2.15).

From the assumption (2.13), we get the nonnegativity of the last coefficients. Therefore, multiplying the first equation of (2.14) by $\dot{\beta}_{ij}$ and the second one by $\sin(\beta_{ij}) \dot{\alpha}_{ij}$, it gives that

$$2 \frac{d\mathcal{A}_{ij}^2}{dt} = \lambda_{ij}^3 |\dot{\beta}_{ij}|^2 + \lambda_{ij}^2 |\sin(\beta_{ij}) \dot{\alpha}_{ij}|^2 \geq 0.$$

Hence, from the nonnegativity of λ_{ij}^2 and λ_{ij}^3 , the result (2.16) follows. \square

Remark 2.10. Notice that (2.16) obtained in Lemma 2.9 ensures that the magnitude of $\mathcal{A}_{ij}^2(t)$ will growth since $(\lambda_{ij}^2, \lambda_{ij}^3)$ given in (2.15) are nonnegative. Furthermore, when λ_{ij}^2 and λ_{ij}^3 are bounded from below, $\mathcal{A}_{ij}^2(t)$ will fast grow exponentially in time.

Applying Lemma 2.9, we observe that we can choose \mathbf{R}_{ij} orthogonal to the unit vector \mathbf{k}_{ij} since this direction does not have any effect on the variation of \mathcal{A}_{ij}^2 . We give a simple choice for \mathbf{R}_{ij} .

Example 2.11. For any frequency $\omega_{ij} > 0$, we take

$$\mathbf{R}_{ij} := -\frac{(\mathbf{v}_j - \mathbf{v}_i) \wedge \mathbf{k}_{ij}}{d_{ij}}$$

and after an easy computation, it gives

$$\begin{cases} r_{ij}^2 = \langle \mathbf{R}_{ij}, \mathbf{e}_{\beta_{ij}} \rangle = -\sin(\beta_{ij}) \dot{\alpha}_{ij}, \\ r_{ij}^3 = \langle \mathbf{R}_{ij}, \mathbf{e}_{\alpha_{ij}} \rangle = \dot{\beta}_{ij}, \end{cases}$$

hence, we have

$$\begin{cases} \frac{d\dot{\beta}_{ij}}{dt} = (2 + \omega_{ij}) \left(\frac{|\mathbf{v}_i - \mathbf{v}_j|}{d_{ij}} \right)^2 \tau_{ij} \dot{\beta}_{ij} + \cos(\beta_{ij}) \sin(\beta_{ij}) \dot{\alpha}_{ij}^2, \\ \frac{d}{dt} (\sin(\beta_{ij}) \dot{\alpha}_{ij}) = (2 + \omega_{ij}) \left(\frac{|\mathbf{v}_i - \mathbf{v}_j|}{d_{ij}} \right)^2 \tau_{ij} \sin(\beta_{ij}) \dot{\alpha}_{ij} - \cos(\beta_{ij}) \dot{\beta}_{ij} \dot{\alpha}_{ij}. \end{cases}$$

Then we have (2.16) with

$$\gamma_{ij} := (2 + \omega_{ij}) \left(\frac{|\mathbf{v}_i - \mathbf{v}_j|}{d_{ij}} \right)^2 \tau_{ij} > 0.$$

2.2.2. Non-cooperative interactions. Consider at $t = t^0$ two particles $(i, j) \in \{1, \dots, N\}^2$ such that $j \in \mathcal{K}_i(t^0)$ but $i \notin \mathcal{K}_j(t^0)$ as it is shown in Figure 4-(b). Then only the particle i will rotate in order to avoid collision along a rotation axis defined by a vector field \mathbf{R}_{ij} which has to be determined such that

$$\begin{cases} \frac{d\mathbf{v}_i}{dt} = \tilde{\omega}_{ij} \mathbf{v}_i \wedge \mathbf{R}_{ij}, \\ \frac{d\mathbf{v}_j}{dt} = 0, \end{cases}$$

where $\tilde{\omega}_{ij} \in \mathbb{R}$. Therefore we apply the same strategy as the one presented below to determine the condition for which the time derivative of the polar angle $\dot{\beta}_{ij}$ and $\sin(\beta_{ij}) \dot{\alpha}_{ij}$ will increase. Hence we prove the following result.

Lemma 2.12. Assume that two particles $(i, j) \in \{1, \dots, N\}^2$ are such that $j \in \mathcal{K}_i(t^0)$ and $i \notin \mathcal{K}_j(t^0)$ and consider the time derivative of the relative bearing and polar angles $(\sin(\beta_{ij}) \dot{\alpha}_{ij}, \dot{\beta}_{ij})$ given in (2.8) and the rotational axis \mathbf{R}_{ij} given by (2.12) is such that $r_{ij}^1 = 0$,

$$(2.17) \quad \tilde{\omega}_{ij} \frac{\cos(\alpha_{ij}) r_{ij}^3}{\dot{\beta}_{ij}} \geq 0 \quad \text{and} \quad \tilde{\omega}_{ij} \frac{\cos(\alpha_{ij}) r_{ij}^2}{\dot{\alpha}_{ij}} \leq 0.$$

Then, $(\sin(\beta_{ij}) \dot{\alpha}_{ij}, \dot{\beta}_{ij})$ is solution to the following system

$$(2.18) \quad \begin{cases} \frac{d\dot{\beta}_{ij}}{dt} = \cos(\beta_{ij}) \sin(\beta_{ij}) \dot{\alpha}_{ij}^2 + \eta_{ij}^3 \dot{\beta}_{ij}, \\ \frac{d}{dt} (\sin(\beta_{ij}) \dot{\alpha}_{ij}) = -\cos(\beta_{ij}) \dot{\alpha}_{ij} \dot{\beta}_{ij} + \eta_{ij}^2 \sin(\beta_{ij}) \dot{\alpha}_{ij}, \end{cases}$$

with

$$\begin{cases} \eta_{ij}^3 := \left(2\tau_{ij} \left(\frac{|\mathbf{v}_j - \mathbf{v}_i|}{d_{ij}} \right)^2 + \tilde{\omega}_{ij} |\mathbf{v}_i| \sin(\beta_{ij}) \frac{\cos(\alpha_{ij}) r_{ij}^3}{\dot{\beta}_{ij}} \right) \in \mathbb{R}^+, \\ \eta_{ij}^2 := \left(2\tau_{ij} \left(\frac{|\mathbf{v}_j - \mathbf{v}_i|}{d_{ij}} \right)^2 - \tilde{\omega}_{ij} |\mathbf{v}_i| \frac{\cos(\alpha_{ij}) r_{ij}^2}{\dot{\alpha}_{ij}} \right) \in \mathbb{R}^+. \end{cases}$$

Furthermore, \mathcal{A}_{ij}^2 given in (2.11) satisfies for $\gamma_{ij} = \min(\eta_{ij}^2, \eta_{ij}^3)$,

$$(2.19) \quad \frac{d\mathcal{A}_{ij}^2}{dt} \geq \frac{\gamma_{ij}}{2} \mathcal{A}_{ij}^2.$$

Proof. We proceed as in the proof of Lemma 2.9, hence we get

$$\frac{d\dot{\beta}_{ij}}{dt} = -\tilde{\omega}_{ij} \frac{\langle \mathbf{v}_i \wedge \mathbf{R}_{ij}, \mathbf{e}_{\beta_{ij}} \rangle}{d_{ij}} + \cos(\beta_{ij}) \sin(\beta_{ij}) \dot{\alpha}_{ij}^2 + 2 \left(\frac{|\mathbf{v}_j - \mathbf{v}_i|}{d_{ij}} \right)^2 \tau_{ij} \dot{\beta}_{ij},$$

and for the time derivative of $\sin(\beta_{ij}) \dot{\alpha}_{ij}$,

$$\frac{d}{dt} (\sin(\beta_{ij}) \dot{\alpha}_{ij}) = -\tilde{\omega}_{ij} \frac{\langle \mathbf{v}_i \wedge \mathbf{R}_{ij}, \mathbf{e}_{\alpha_{ij}} \rangle}{d_{ij}} - \cos(\beta_{ij}) \dot{\beta}_{ij} \dot{\alpha}_{ij} + 2 \left(\frac{|\mathbf{v}_j - \mathbf{v}_i|}{d_{ij}} \right)^2 \tau_{ij} \sin(\beta_{ij}) \dot{\alpha}_{ij}.$$

Furthermore, from the expression of $\mathbf{e}_{\beta_{ij}}$ and $\mathbf{e}_{\alpha_{ij}}$ in (2.7) and choosing $r_{ij}^1 = 0$, we get that

$$\begin{cases} \langle \mathbf{v}_i \wedge \mathbf{R}_{ij}, \mathbf{e}_{\beta_{ij}} \rangle = -r_{ij}^3 \langle \mathbf{v}_i, \mathbf{k}_{ij} \rangle = -|\mathbf{v}_i| \cos(\alpha_{ij}) \sin(\beta_{ij}) r_{ij}^3, \\ \langle \mathbf{v}_i \wedge \mathbf{R}_{ij}, \mathbf{e}_{\alpha_{ij}} \rangle = +r_{ij}^2 \langle \mathbf{v}_i, \mathbf{k}_{ij} \rangle = +|\mathbf{v}_i| \cos(\alpha_{ij}) \sin(\beta_{ij}) r_{ij}^2. \end{cases}$$

It gives the following system of equations

$$\begin{cases} \frac{d\dot{\beta}_{ij}}{dt} = \cos(\beta_{ij}) \sin(\beta_{ij}) \dot{\alpha}_{ij}^2 + \left(2\tau_{ij} \left(\frac{|\mathbf{v}_j - \mathbf{v}_i|}{|\mathbf{x}_j - \mathbf{x}_i|} \right)^2 + \tilde{\omega}_{ij} |\mathbf{v}_i| \sin(\beta_{ij}) \frac{\cos(\alpha_{ij}) r_{ij}^3}{\dot{\beta}_{ij}} \right) \dot{\beta}_{ij}, \\ \frac{d}{dt} (\sin(\beta_{ij}) \dot{\alpha}_{ij}) = -\cos(\beta_{ij}) \dot{\alpha}_{ij} \dot{\beta}_{ij} + \left(2\tau_{ij} \left(\frac{|\mathbf{v}_j - \mathbf{v}_i|}{|\mathbf{x}_j - \mathbf{x}_i|} \right)^2 - \tilde{\omega}_{ij} |\mathbf{v}_i| \frac{\cos(\alpha_{ij}) r_{ij}^2}{\dot{\alpha}_{ij}} \right) \sin(\beta_{ij}) \dot{\alpha}_{ij}. \end{cases}$$

From the assumption (2.17), we get the nonnegativity of the last coefficients. Therefore, multiplying the first equation of (2.18) by $\dot{\beta}_{ij}$ and the second one by $\sin(\beta_{ij}) \dot{\alpha}_{ij}$, it gives that

$$2 \frac{d\mathcal{A}_{ij}^2}{dt} = \eta_{ij}^3 |\dot{\beta}_{ij}|^2 + \eta_{ij}^2 |\sin(\beta_{ij}) \dot{\alpha}_{ij}|^2 \geq 0,$$

hence (2.19) follows with $\gamma_{ij} = \min(\eta_{ij}^2, \eta_{ij}^3)$. \square

Following Example 2.11, we give a simple choice for \mathbf{R}_{ij} .

Example 2.13. For any frequency $\omega_{ij} > 0$, we choose $\tilde{\omega}_{ij} = \omega_{ij} \cos(\alpha_{ij})$ and \mathbf{R}_{ij} such that

$$\mathbf{R}_{ij} := -\frac{(\mathbf{v}_j - \mathbf{v}_i) \wedge \mathbf{k}_{ij}}{d_{ij}}$$

and as in Example 2.11 we get

$$\begin{cases} r_{ij}^2 = \langle \mathbf{R}_{ij}, \mathbf{e}_{\beta_{ij}} \rangle = -\sin(\beta_{ij}) \dot{\alpha}_{ij}, \\ r_{ij}^3 = \langle \mathbf{R}_{ij}, \mathbf{e}_{\alpha_{ij}} \rangle = \dot{\beta}_{ij}. \end{cases}$$

Hence, from the choice of $\tilde{\omega}_{ij}$ and the latter equalities, the assumption (2.17) is satisfied, then we can apply Lemma 2.12 and the particle $i \in \{1, \dots, N\}$ will deviate from $j \in \mathcal{K}_i(t^0)$ whereas j will continue its free motion.

2.2.3. *Collision avoidance model.* Finally, taking into account all the interactions between particles at time $t = t^0$, the force field applied for collision avoidance is given by the sum of interactions as

$$(2.20) \quad \mathbf{F}_i^{\text{self}}(\mathbf{x}_i, \mathbf{v}_i) = \frac{1}{N} \sum_{j=1}^N \omega_{ij} H_{ij} \mathbf{1}_{\mathcal{K}_i(t^0)}(j) \mathbf{v}_i \wedge \mathbf{R}_{ij},$$

where $\mathbf{1}_{\mathcal{K}_i(t^0)}$ represents the characteristic function of the set $\mathcal{K}_i(t^0)$ defined in (2.5), $\omega_{ij} > 0$ and the rotational axis \mathbf{R}_{ij} is given by

$$(2.21) \quad \mathbf{R}_{ij} := -\frac{(\mathbf{v}_j - \mathbf{v}_i) \wedge \mathbf{k}_{ij}}{d_{ij}},$$

whereas the function H_{ij} corresponds to either cooperative or non-cooperative actions as explained above,

$$(2.22) \quad H_{ij} = \begin{cases} 1, & \text{if } i \in \mathcal{K}_j(t^0), \\ \cos(\alpha_{ij}), & \text{else.} \end{cases}$$

In the sequel the frequency $\omega_{ij} > 0$ is chosen such that ω_{ij} tends to zero when $\tau_{ij} \rightarrow +\infty$,

$$(2.23) \quad \omega_{ij} = \frac{8\pi}{|\mathbf{R}_{ij}|} e^{-\tau_{ij}}.$$

Remark 2.14. Note that in some particular cases even when the set $\mathcal{K}_i(t)$ is not empty, the force term $\mathbf{F}_i^{\text{self}}(\mathbf{x}_i, \mathbf{v}_i)$ may be zero. Indeed, it happens for instance

- when \mathbf{k}_{ij} is colinear to $\mathbf{v}_j - \mathbf{v}_i$, hence the vector $\mathbf{R}_{ij} = 0$,
- or when the location of the set particles in the vision cone of i are perfectly symmetric with respect to the axis passing by \mathbf{x}_i of direction \mathbf{v}_i , hence $\mathbf{F}_i^{\text{self}}(\mathbf{x}_i, \mathbf{v}_i)$.

Therefore, in that case we choose it as

$$\mathbf{F}_i^{\text{self}}(\mathbf{x}_i, \mathbf{v}_i) = \frac{\varepsilon}{N} \sum_{j=1}^N e^{-\tau_{ij}} H_{ij} \mathbf{1}_{\mathcal{K}_i(t^0)}(j) \mathbf{v}_i \wedge \mathbf{e}_z,$$

where ε is chosen randomly and of order 10^{-6} . In practice this force term allows to break the symmetry and to remove the degeneracy.

2.3. **Avoidance of obstacles and influence of the target.** Using the same strategy as the one described below, obstacles $O \subset \mathbb{R}^3$ are treated as particles, where the particle interacts with the closest point belonging to the intersection of the obstacle and the vision cone of the particle i at time t^0 ,

$$\mathbf{x}_O = \arg \min_{\mathbf{x} \in \partial O \cap \mathcal{K}_i(t^0)} d(\mathbf{x}_i(t^0), \mathbf{x}),$$

whereas $\mathbf{v}_0 \in \mathbb{R}^3$ is the given velocity of the obstacle. Then the collision avoidance follows the same process as before except that the obstacle does not deviate.

On the other hand, a force $-\nabla V(\mathbf{x}_i)$ is applied to steer particle i to its destination. The potential V is the distance function

$$V(\mathbf{x}_i) = |\mathbf{x}_i - \mathbf{x}_T|,$$

where \mathbf{x}_T represents the location of the target, whereas a friction term is added to control the speed of the particle $i \in \{1, \dots, N\}$. Hence the particle i is directed by the sum of the gradient of the potential field $-\nabla V(\mathbf{x}_i)$ and the friction force in the following manner

$$\mathbf{F}_i^{\text{ext}}(\mathbf{x}_i, \mathbf{v}_i) = -\nabla V(\mathbf{x}_i) - \sigma \mathbf{v}_i,$$

where $\sigma > 0$ represents the friction coefficient. This latter force field induces a change of speed of particle $(\mathbf{x}_i, \mathbf{v}_i)$.

2.4. Influence of the noise. Obviously, the motion of particles is not fully deterministic. When some decisions need to be made in front of several alternatives, the response of the subjects is subject-dependent. The simplest way to model this inherent uncertainty consists in adding a Brownian motion in velocity [27]

$$d\mathbf{v}_i = \sqrt{2\nu} \circ dB_t^i,$$

where $\sqrt{2\nu}$ is the noise intensity and where dB_t^i are standard white noises in 3D, which are independent from one particle to another one. The circle means that the stochastic differential equation must be understood in the Stratonovich sense. The integration of this stochastic differential equation generates a Brownian motion [24, 27]. This stochastic term adds up to the previous ones.

2.5. Agent-based model for collision avoidance. Finally from the requirements defined in the perception and decision making phases, we get the following model constructed from the force field $\mathbf{F}_i^{\text{self}}$ and $\mathbf{F}_i^{\text{ext}}$,

$$(2.24) \quad \begin{cases} \frac{d\mathbf{x}_i}{dt} = \mathbf{v}_i, \\ d\mathbf{v}_i = \left(\frac{1}{N} \sum_{j=1}^N \omega_{ij} H_{ij} \mathbf{1}_{\mathcal{K}_i(t)}(j) \mathbf{v}_i \wedge \mathbf{R}_{ij} - \nabla V(\mathbf{x}_i) - \sigma \mathbf{v}_i \right) dt + \sqrt{2\nu} \circ dB_t^i, \end{cases}$$

where \mathbf{R}_{ij} , H_{ij} and ω_{ij} are given in (2.21)-(2.23).

Note that in the two dimensional case, the interactions occur in the horizontal plane and the rotation axis is parallel to Oz , hence we recover the model proposed for pedestrian in [9, 10] for binary interactions. However, for multiple interactions the models differ since in our approach, the particle i only rotates to avoid collision among other particles without optimizing its trajectory to reach a target as in [9, 10]. In (2.24), interacting particles are considered as obstacles where the intensity of the force depends on the time to interaction τ_{ij} thanks to the frequency ω_{ij} in (2.23) : the probability to deviate is small when τ_{ij} is high and is of order one when $\tau_{ij} \rightarrow 0$. This principle can be viewed as an instantaneous reaction to avoid collision with particles around.

Proposition 2.15. *Consider the solution $(\mathbf{x}_i, \mathbf{v}_i)_{1 \leq i \leq N}$ to the agent-based model (2.24) without noise ($\nu = 0$). Then the energy given by*

$$\mathcal{E}(t) := \sum_{i=1}^N \left(\frac{|\mathbf{v}_i|^2}{2} + V(\mathbf{x}_i) \right),$$

satisfies the following estimate

$$\frac{d\mathcal{E}}{dt} \leq - \sum_{i=1}^N \sigma |\mathbf{v}_i|^2.$$

Proof. Simply multiply the second equation of (2.24) by \mathbf{v}_i and integrate by part. By orthogonality property, we get the energy estimate. \square

3. MEAN FIELD KINETIC MODEL

We now consider the limit of a large number of particles $N \rightarrow \infty$. We will give a formal proof of convergence when there is no noise $\nu = 0$ dealing with dynamical systems with discontinuous coefficients and then with noise dealing with stochastic differential systems.

3.1. Mean field model without noise. We first consider the case without noise. For this derivation, we proceed like in [31]. We introduce the so-called empirical distribution $f^N(t, \mathbf{x}, \mathbf{v})$ defined by

$$f^N(t, \mathbf{x}, \mathbf{v}) := \frac{1}{N} \sum_{i=1}^N \delta(\mathbf{x} - \mathbf{x}_i) \delta(\mathbf{v} - \mathbf{v}_i),$$

where $(\mathbf{x}_i, \mathbf{v}_i)_{1 \leq i \leq N}$ is solution to the system of ODEs (2.24) with $\nu = 0$.

We introduce the cone $\mathcal{C}(\mathbf{v})$ centered at the origin, with angle $\cos^{-1}(\kappa)$, $\kappa \in [-1, 1]$ about the direction $\mathbf{v} \in \mathbb{R}^3$

$$\mathcal{C}(\mathbf{v}) := \{ \mathbf{z} \in \mathbb{R}^3, \quad \langle \mathbf{z}, \mathbf{v} \rangle \geq \kappa |\mathbf{z}| |\mathbf{v}| \}$$

and for any $\mathbf{u} \in \mathbb{R}^3$, we set $\mathcal{I}(\mathbf{u})$ as

$$\mathcal{I}(\mathbf{u}) := \{ \mathbf{z} \in \mathbb{R}^3, \quad \tau(\mathbf{z}, \mathbf{u}) > 0, \quad D(\mathbf{z}, \mathbf{u}) \leq R \},$$

where the functions D and τ correspond to

$$(3.25) \quad \begin{cases} D(\mathbf{z}, \mathbf{u}) = \left(|\mathbf{z}|^2 - \left(\mathbf{z} \cdot \frac{\mathbf{u}}{|\mathbf{u}|} \right)^2 \right)^{1/2}, \\ \tau(\mathbf{z}, \mathbf{u}) = -\frac{\mathbf{z} \cdot \mathbf{u}}{|\mathbf{u}|^2}. \end{cases}$$

Finally, we define $\mathcal{K}(\mathbf{v}, \mathbf{w}) \subset \mathbb{R}^3$ as

$$\mathcal{K}(\mathbf{v}, \mathbf{w}) = \mathcal{I}(\mathbf{w} - \mathbf{v}) \cap \mathcal{C}(\mathbf{v}).$$

Then, it is an easy matter to see that f^N satisfies the following kinetic equation in the distribution sense

$$(3.26) \quad \partial_t f^N + \mathbf{v} \cdot \nabla_{\mathbf{x}} f^N - \nabla_{\mathbf{x}} V \cdot \nabla_{\mathbf{v}} f^N + \nabla_{\mathbf{v}} \cdot (\mathbf{v} \wedge \Omega^N f^N) = \sigma \nabla_{\mathbf{v}} \cdot (\mathbf{v} f^N),$$

where $\Omega^N(t, \mathbf{x}, \mathbf{v})$ is an interaction force defined by

$$(3.27) \quad \Omega^N(t, \mathbf{x}, \mathbf{v}) = -\frac{1}{N} \sum_{j=1}^N m(\mathbf{x}_j - \mathbf{x}, \mathbf{v}, \mathbf{v}_j) \mathbb{1}_{\mathcal{K}(\mathbf{v}, \mathbf{v}_j)}(\mathbf{x}_j - \mathbf{x}) \mathbf{R}(\mathbf{x}_j - \mathbf{x}, \mathbf{v}_j - \mathbf{v}),$$

with the rotation axis $\mathbf{R}(\mathbf{z}, \mathbf{u})$ given by

$$\mathbf{R}(\mathbf{z}, \mathbf{u}) = \frac{\mathbf{u} \wedge \mathbf{z}}{|\mathbf{z}|^2},$$

whereas the scalar function m takes into account the frequency and the cooperative and non-cooperative interaction,

$$m(\mathbf{z}, \mathbf{v}, \mathbf{w}) = \frac{8\pi}{|\mathbf{R}(\mathbf{z}, \mathbf{w} - \mathbf{v})|} H_{\mathcal{C}(\mathbf{w})}(\mathbf{z}, \mathbf{v}) e^{-\tau(\mathbf{z}, \mathbf{w} - \mathbf{v})},$$

where

$$H_{\mathcal{C}(\mathbf{w})}(\mathbf{z}, \mathbf{v}) = \begin{cases} 1, & \text{if } \mathbf{z} \in \mathcal{C}(\mathbf{w}), \\ \cos(\alpha(\mathbf{z}, \mathbf{v})), & \text{else,} \end{cases}$$

where $\alpha(\mathbf{z}, \mathbf{v}) \in (0, 2\pi)$ corresponds to the relative azimuthal angle of \mathbf{z} in the frame constructed from \mathbf{v} written in spherical coordinates $\{\mathbf{e}_{|\mathbf{v}|}, \mathbf{e}_\phi, \mathbf{e}_\theta\}$.

We note that relation (3.27) can be written

$$(3.28) \quad \Omega^N(t, \mathbf{x}, \mathbf{v}) = - \int_{\mathbb{R}^3 \times \mathbb{R}^3} m(\mathbf{z}, \mathbf{v}, \mathbf{w}) \mathbb{1}_{\mathcal{K}(\mathbf{v}, \mathbf{w})}(\mathbf{z}) \mathbf{R}(\mathbf{z}, \mathbf{w} - \mathbf{v}) f^N(t, \mathbf{x} + \mathbf{z}, \mathbf{w}) d\mathbf{z} d\mathbf{w},$$

which is a convolution product with respect to the space variable $\mathbf{x} \in \mathbb{R}^3$. Clearly, the formal mean-field limit of the particle system modeled by the kinetic system (3.26), (3.28) is given by the following

system:

$$(3.29) \quad \begin{cases} \partial_t f + \mathbf{v} \cdot \nabla_{\mathbf{x}} f - \nabla_{\mathbf{x}} V \cdot \nabla_{\mathbf{v}} f + \nabla_{\mathbf{v}} \cdot (\mathbf{v} \wedge \Omega_f f) = \sigma \nabla_{\mathbf{v}} \cdot (\mathbf{v} f), \\ \Omega_f(\mathbf{x}, \mathbf{v}) = - \int_{\mathbb{R}^3 \times \mathbb{R}^3} m(\mathbf{z}, \mathbf{v}, \mathbf{w}) \mathbf{1}_{\mathcal{K}(\mathbf{v}, \mathbf{w})}(\mathbf{z}) \mathbf{R}(\mathbf{z}, \mathbf{w} - \mathbf{v}) f(t, \mathbf{x} + \mathbf{z}, \mathbf{w}) d\mathbf{z} d\mathbf{w}, \\ f(t=0) = f_0 \in \mathcal{P}_1 \cap L^\infty(\mathbb{R}^6), \end{cases}$$

where we denote by $\mathcal{P}_1(\mathbb{R}^6)$, the set of probability measures in \mathbb{R}^6 with first bounded moment, which is a complete metric space endowed with the Monge-Kantorovich-Rubinstein distance. The Monge-Kantorovich-Rubinstein distance, also called 1-Wasserstein distance, is also equivalent to the Bounded Lipschitz distance

$$d_1(f, g) = \sup \left\{ \left| \int_{\mathbb{R}^6} \varphi(\mathbf{z}) df(\mathbf{z}) - \int_{\mathbb{R}^6} \varphi(\mathbf{z}) dg(\mathbf{z}) \right|, \varphi \in \text{Lip}(\mathbb{R}^6), \text{Lip}(\varphi) \leq 1 \right\},$$

where $\text{Lip}(\mathbb{R}^6)$ denotes the set of Lipschitz functions on \mathbb{R}^6 and $\text{Lip}(\varphi)$ respectively the Lipschitz constant of a function φ .

It is an open problem to rigorously show that this convergence holds. On the one hand, the lack of regularity of the velocity field in (2.24), due to the sharpness of the sensitivity regions \mathcal{K}_i given in (2.5), prevents classical arguments from deriving rigorously the mean-field limit. We refer to the recent work in [5], where the authors show the rigorous proof of the mean-field limit of a system of interacting particles where each particle only interacts with those inside a local region whose shape depends on the position and velocity of the particle. The argument is based on Filippov's theory [16] allowing to have a well-defined notion of solutions via differential inclusions. On the other hand, the additional work to take care concerns the control of the error term in d_1 between weak solutions to (3.29) and empirical measures associated to differential inclusions to (2.24).

Suppose that the empirical measure f^N at time $t = 0$ converges in the weak star topology of bounded measures towards a smooth function f_0 such that

$$d_1(f^N(0), f_0) \rightarrow 0, \quad \text{when } N \rightarrow \infty.$$

Following [5], we may define the solution $f^N(t)$ to (3.26) and $f(t)$ to (3.29) thanks to the theory of characteristics, hence it remains to establish a stability estimate as

$$d_1(f^N(t), f(t)) \leq e^{Ct} d_1(f^N(0), f_0), \quad \forall t \in [0, T],$$

where $C > 0$ is a positive constant depending on f . We will admit that such a result is true and leave a rigorous convergence proof to future work following [5].

For (3.29) we can prove an analogous property as Proposition 2.15 for (2.24)

Theorem 3.1. *Consider a smooth potential $V(\mathbf{z}) \geq 0$ and $V \in \mathcal{C}^1(\mathbb{R}^3)$. Assume that $f_0 \in L^1 \cap L^\infty(\mathbb{R}^6)$, with $f_0 \geq 0$ and*

$$\int_{\mathbb{R}^6} (|\mathbf{x}|^2 + |\mathbf{v}|^2) f_0(\mathbf{x}, \mathbf{v}) d\mathbf{x} d\mathbf{v} < \infty.$$

Then for any $T > 0$, there exists a weak solution to (3.29) such that for almost every $t \in [0, T]$,

$$f(t) \in L^1 \cap L^\infty(\mathbb{R}^6), \quad \int_{\mathbb{R}^6} (|\mathbf{x}|^2 + |\mathbf{v}|^2) f(t, \mathbf{x}, \mathbf{v}) d\mathbf{x} d\mathbf{v} < C(T, f_0)$$

and for any $\varphi \in \mathcal{C}_c^\infty([0, T] \times \mathbb{R}^6)$,

$$(3.30) \quad \int_0^T \int_{\mathbb{R}^6} f(t) (\partial_t \varphi + \mathbf{v} \cdot \nabla_{\mathbf{x}} \varphi - (\nabla_{\mathbf{x}} V - \mathbf{v} \wedge \Omega_f + \sigma \mathbf{v}) \cdot \nabla_{\mathbf{v}} \varphi) d\mathbf{x} d\mathbf{v} dt + \int_{\mathbb{R}^6} f_0 \varphi(0) d\mathbf{x} d\mathbf{v} = 0.$$

Moreover, we have

$$\frac{d}{dt} \int_{\mathbb{R}^6} \left(\frac{|\mathbf{v}|^2}{2} + V(\mathbf{x}) \right) f(t, \mathbf{x}, \mathbf{v}) d\mathbf{x} d\mathbf{v} \leq -\sigma \int_{\mathbb{R}^6} |\mathbf{v}|^2 f(t, \mathbf{x}, \mathbf{v}) d\mathbf{x} d\mathbf{v}$$

Proof. We only give *a priori* estimates which allow to prove existence of solutions by applying a classical regularizing process by convolution.

We consider a smooth solution to (3.29), which is a six dimensional advection equation in conservative form, hence we get conservation of mass and nonnegativity of the solution leading to

$$\|f(t)\|_{L^1} = \|f_0\|_{L^1}, \quad \forall t \in [0, T].$$

From this estimate and since $m(\mathbf{z}, \mathbf{v}, \mathbf{w}) |\mathbf{R}(\mathbf{z}, \mathbf{w} - \mathbf{v})| \leq 1$, for any $\mathbf{z} \in \mathcal{K}(\mathbf{v}, \mathbf{w})$, we prove that

$$\|\Omega_f\|_{L^\infty} \leq \|f(t)\|_{L^1} = \|f_0\|_{L^1}, \quad \forall t \in [0, T].$$

Furthermore, since the advection field is locally bounded in L^∞ , for any $p > 1$, we multiply (3.29) by $p|f|^{p-1}$ and integrate over $(\mathbf{x}, \mathbf{v}) \in \mathbb{R}^6$. It yields to the existence of a constant $C > 0$ depending on $\|f_0\|_{L^1}$ such that

$$\|f(t)\|_{L^p} = \|f_0\|_{L^p} e^{Ct}, \quad \forall t \in [0, T].$$

Next we multiply (3.29) by $\frac{1}{2}|\mathbf{v}|^2 + V(\mathbf{x})$ and integrate over $(\mathbf{x}, \mathbf{v}) \in \mathbb{R}^6$. After an integration by part, we get

$$\frac{d}{dt} \int_{\mathbb{R}^6} \left(\frac{|\mathbf{v}|^2}{2} + V(\mathbf{x}) \right) f(t, \mathbf{x}, \mathbf{v}) d\mathbf{x} d\mathbf{v} \leq -\sigma \int_{\mathbb{R}^6} |\mathbf{v}|^2 f(t, \mathbf{x}, \mathbf{v}) d\mathbf{x} d\mathbf{v},$$

which allows to control the following quantity $|\mathbf{v}|^2 f(t)$ in $L^1(\mathbb{R}^6)$. Finally, we multiply (3.29) by $|\mathbf{x}|^2$ and integrate over $(\mathbf{x}, \mathbf{v}) \in \mathbb{R}^6$,

$$\begin{aligned} \frac{d}{dt} \int_{\mathbb{R}^6} |\mathbf{x}|^2 f(t, \mathbf{x}, \mathbf{v}) d\mathbf{x} d\mathbf{v} &= 2 \int_{\mathbb{R}^6} \mathbf{x} \cdot \mathbf{v} f(t, \mathbf{x}, \mathbf{v}) d\mathbf{x} d\mathbf{v}, \\ &\leq 2 \left(\int_{\mathbb{R}^6} |\mathbf{x}|^2 f(t, \mathbf{x}, \mathbf{v}) d\mathbf{x} d\mathbf{v} \right)^{1/2} \left(\int_{\mathbb{R}^6} |\mathbf{v}|^2 f(t, \mathbf{x}, \mathbf{v}) d\mathbf{x} d\mathbf{v} \right)^{1/2}, \end{aligned}$$

hence we get the estimate on the second order moment in space thanks to the previous results.

Finally, from these *a priori* estimates, we get enough compactness to pass to the limit in a regularized problem in the nonlinear term $f(t) \mathbf{v} \wedge \Omega_f$ in (3.30) and prove existence of weak solutions on any finite time interval $[0, T]$. \square

Next, from the kinetic equation (3.29), we can construct an hydrodynamical system by considering a mono-kinetic approximation given by

$$f(t, \mathbf{x}, \mathbf{v}) = \rho(t, \mathbf{x}) \delta(\mathbf{v} - \mathbf{U}(t, \mathbf{x})),$$

hence the couple (ρ, \mathbf{U}) is solution to

$$\begin{cases} \partial_t \rho + \nabla_{\mathbf{x}} \cdot (\rho \mathbf{U}) = 0, \\ \partial_t \rho \mathbf{U} + \nabla_{\mathbf{x}} \cdot (\rho \mathbf{U} \otimes \mathbf{U}) = -\nabla_{\mathbf{x}} V \rho + \rho \mathbf{U} \wedge \Omega - \sigma \rho \mathbf{U}, \end{cases}$$

where Ω is given by

$$\Omega(t, \mathbf{x}) = - \int_{\mathbb{R}^3} m(\mathbf{z}, \mathbf{U}(t, \mathbf{x}), \mathbf{U}(t, \mathbf{x} + \mathbf{z})) \mathbb{1}_{\mathcal{K}(\mathbf{U}(t, \mathbf{x}), \mathbf{U}(t, \mathbf{x} + \mathbf{z}))}(\mathbf{z}) \mathbf{R}(\mathbf{z}, \mathbf{U}(t, \mathbf{x} + \mathbf{z}), \mathbf{U}(t, \mathbf{x})) \rho(\mathbf{x} + \mathbf{z}) d\mathbf{z}.$$

3.2. Mean field model with noise. We now consider the case (2.24) with Gaussian noise $\nu > 0$. This problem has been addressed in [1], where the authors show that the N interacting processes $(\mathbf{x}_{i,t}, \mathbf{v}_{i,t})_{t \geq 0}$ respectively behave as $N \rightarrow \infty$ like the auxiliary processes $(\bar{\mathbf{x}}_{i,t}, \bar{\mathbf{v}}_{i,t})_{t \geq 0}$, solutions to

$$(3.31) \quad \begin{cases} d\mathbf{x}_{i,t} = \mathbf{v}_{i,t} dt, \\ d\mathbf{v}_{i,t} = (\mathbf{v}_{i,t} \wedge \Omega_{f_t}(\mathbf{x}_{i,t}, \mathbf{v}_{i,t}) - \nabla V(\mathbf{x}_{i,t}) - \sigma \mathbf{v}_{i,t}) dt + \sqrt{2\nu} \circ dB_t^i, \end{cases}$$

where $f_t := \text{law}(\mathbf{x}_{i,t}, \mathbf{v}_{i,t})$ and

$$\Omega_{f_t}(\mathbf{x}_{i,t}, \mathbf{v}_{i,t}) = - \int_{\mathbb{R}^3 \times \mathbb{R}^3} m(\mathbf{z}, \mathbf{v}_{i,t}, \mathbf{w}) \mathbb{1}_{\mathcal{K}(\mathbf{v}_{i,t}, \mathbf{w})}(\mathbf{z}) \mathbf{R}(\mathbf{z}, \mathbf{w} - \mathbf{v}_{i,t}) f(t, \mathbf{x} + \mathbf{z}, \mathbf{w}) d\mathbf{z} d\mathbf{w}.$$

Note that (3.31) consists of N equations which can be solved independently of each other. Each of them involves the condition that f_t is the distribution of $(\mathbf{x}_{i,t}, \mathbf{v}_{i,t})$, thus making it nonlinear. The

processes $(\mathbf{x}_{i,t}, \mathbf{v}_{i,t})_{t \geq 0}$ with $i \in \{1, \dots, N\}$ are independent since the initial conditions and driving Brownian motions are independent.

We will admit that these processes defined on \mathbb{R}^6 are identically distributed, and their common law f_t at time t , as a measure on $\mathbb{R}^3 \times \mathbb{R}^3$ evolves according to the following Kolmogorov-Fokker-Planck equation

$$(3.32) \quad \partial_t f + \mathbf{v} \cdot \nabla_{\mathbf{x}} f - \nabla_{\mathbf{x}} V \cdot \nabla_{\mathbf{v}} f + \nabla_{\mathbf{v}} \cdot (\mathbf{v} \wedge \Omega_f f) = \nabla_{\mathbf{v}} \cdot (\nu \nabla_{\mathbf{v}} f + \sigma \mathbf{v} f).$$

4. NUMERICAL EXPERIMENTS

In this section we present simulations to show the effectiveness of the collision avoidance procedure proposed in this paper at the microscopic level (2.24) with (2.21)-(2.23).

We choose a smooth external potential V such that

$$V(\mathbf{x}) = \frac{1}{4} (1 + |\mathbf{x} - \mathbf{x}_T|^2)^{1/2}$$

and the friction coefficient is fixed to $\sigma = 1/4$. Furthermore to emphasize the effect of the collision avoidance process we neglect the noise and set $\nu = 0$ in our simulations.

4.1. Collision avoidance in the horizontal plane. We first consider the simple situation where all particles move in a direction parallel to the horizontal plane. Initially, all the particles are located in a circle and want to move on the opposite direction with an initial velocity $\mathbf{v}(0) = -\mathbf{x}(0)/2$. Therefore in this very specific situation, the collision point of all particles is the center of the circle.

We consider the microscopic model (2.24) without any noise $\nu = 0$ and choose the radius of the circle delimiting the safety region as depicted in Figure 1 such that $R = 1$. For the vision cone given in Definition 2.5 we take $\kappa = \cos(2\pi/3)$ whereas the axis of rotation and the turning frequency are given in (2.20)-(2.23). Since the motion occurs in the horizontal plane, we expect the axis of rotation r_{ij} to be colinear to the unit vector \mathbf{e}_z . In Figure 5, we present the numerical results with two, three, four and nine particles and observe that the present model preserves perfectly the symmetry. Furthermore, due to the perception phase, the collision is anticipated which seems to guarantee a smooth trajectory and not a brutal change of direction.

These numerical results reproduce the classical trajectories as in [30]. The particles move in a straight line to its own target, then when it approaches the collision point, it starts to rotate and finally deviates again to reach the target point.

Furthermore, we illustrate the fact that in some situations, collision cannot be avoided in particular when the relative velocity between interacting particles is too large, that is, the distance between two interacting particles maybe very small. For instance, we consider the previous situation with three particles localized on the unit circle but now we vary the modulus of the initial velocity $\mathbf{v}(0) = -\alpha \mathbf{x}(0)$, with respect to $\alpha > 0$. The results are presented in Figure 6, as it is expected when the velocity of particles is too large, the distance between particles becomes smaller and smaller.

4.2. Influence of the vision cone. We still consider the motion in the horizontal plane, but now the particles are almost aligned to the Ox axis and move initially along this line where the particle behind has a larger speed than the one in front of it, that is, for a small parameter $\epsilon = 10^{-6}$, we choose $\mathbf{x}_1(0) = (-4, \epsilon, 0)$ and $\mathbf{v}_1(0) = (1, 0, 0)$, whereas $\mathbf{x}_2(0) = (-2, 0, 0)$ and $\mathbf{v}_2(0) = (1/2, 0, 0)$.

Furthermore, for each particle the target is also on the same line. Thus, it is expected that the particle $(\mathbf{x}_1, \mathbf{v}_1)$ turns in order to avoid a collision with $(\mathbf{x}_2, \mathbf{v}_2)$ whereas due to the restriction of the vision cone, the second particle does not see the first one, hence it continues its cruise in a straight line.

Finally we also consider the same situation with three particles with $\mathbf{x}_3(0) = (-6, 2\epsilon, 0)$ and $\mathbf{v}_3(0) = (2, 0, 0)$.

We present the numerical experiment in Figure 7 for two and three particles. In the first situation, we observe that indeed the first particle deviates in order to avoid the collision, whereas in the presence of three particles, the first one deviates much more in order to avoid the collision with the second and

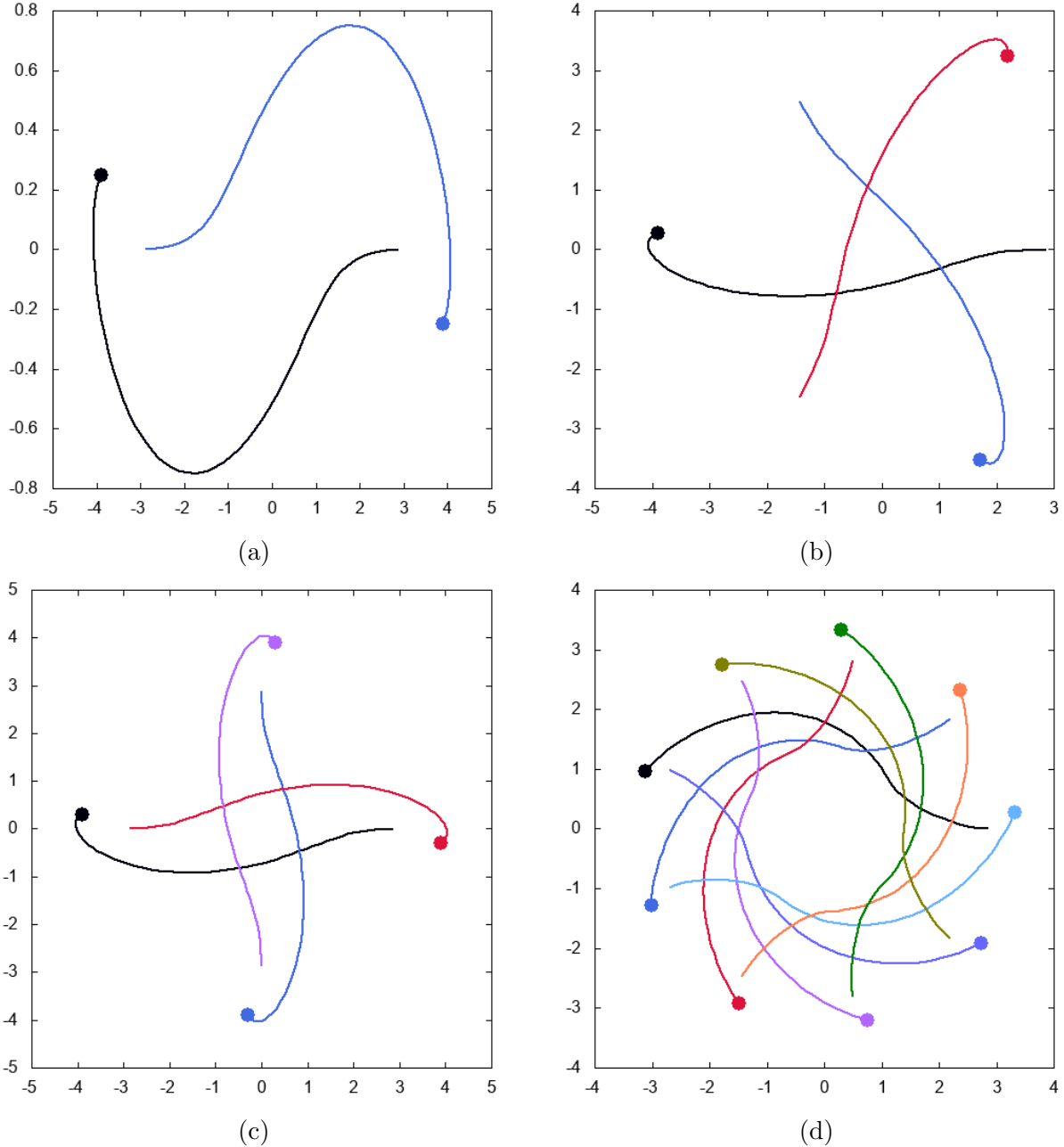


FIGURE 5. **Collision avoidance in the horizontal plan.** space trajectory in the horizontal plane for (a) 2 particles, (b) 3 particles, (c) 4 particles and (d) 9 particles.

the third ones. The particle located in the front does not see the other one coming from behind and does not deviate. This is a simple illustration of the influence of the vision's cone.

4.3. Collision avoidance in 3D. We then consider the situation where all particles move in a three dimensional space. All the particles are initially located in a ball and want to move on the opposite direction with respect to the center of the ball. Therefore in this situation, the collision point of all particles is the center of the ball.

We consider the microscopic model (2.24) without any noise $\nu = 0$ and choose $R = 1$, and for the vision cone given in Definition 2.5 we take $\kappa = \cos(2\pi/3)$ whereas the rotation axis and the turning frequency are given in (2.20)-(2.23).

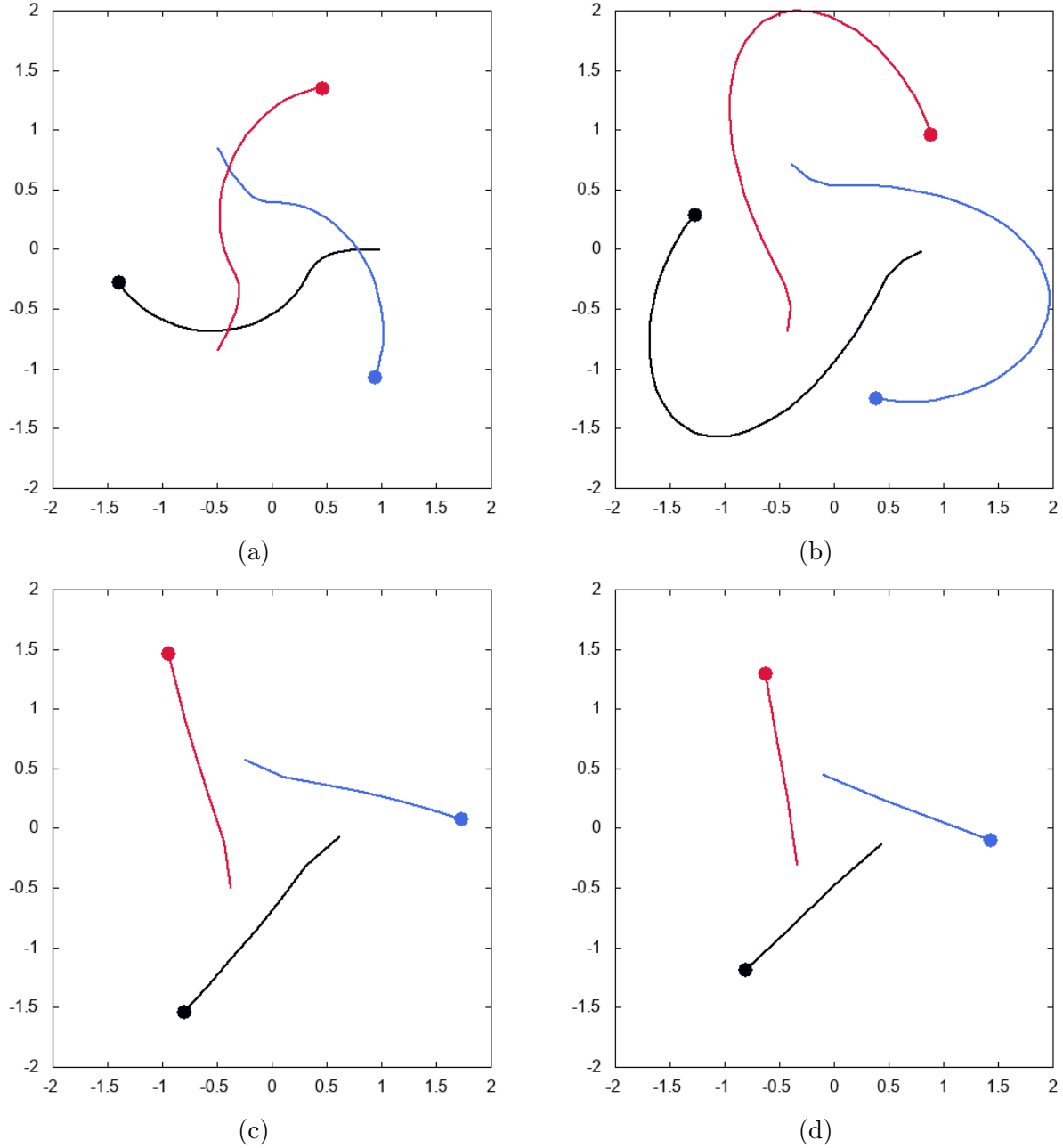


FIGURE 6. **Collision avoidance in the horizontal plan.** space trajectory in the horizontal plane for three particles with different initial velocities (a) $\mathbf{v}(0) = -\mathbf{x}(0)/10$, (b) $\mathbf{v}(0) = -\mathbf{x}(0)$, (c) $\mathbf{v}(0) = -2\mathbf{x}(0)$ and (d) $\mathbf{v}(0) = -3\mathbf{x}(0)$.

In that case we recover a situation similar to the previous one but in three dimensions and the rotation axis is no more colinear to the \mathbf{e}_z unit vector. Thanks to the turning operator, the collision is avoided and the particles have a smooth trajectory in 3D as it can be shown in Figure 8 for two or three particles. With more particles we recover the same kind of results as for the motion in the horizontal plane.

4.4. Moving around obstacles. In this last example, we consider the motion of particles in presence of fixed obstacles. The collision avoidance process follows the line of Section 2.2.2 with non-cooperative

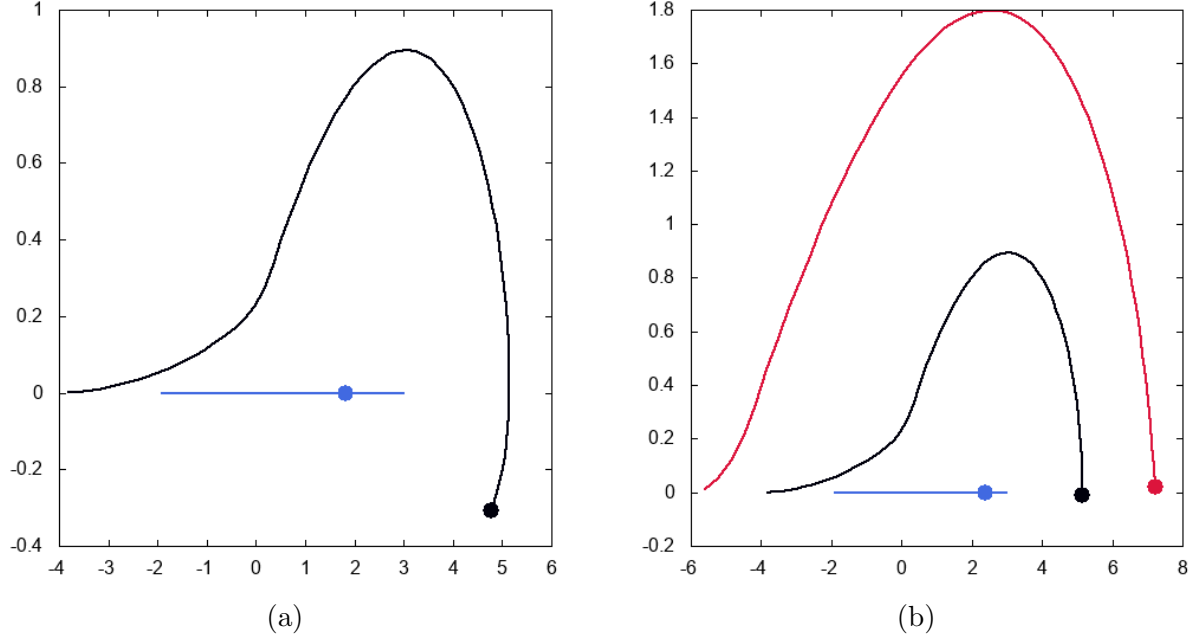


FIGURE 7. **Influence of the vision's cone.** space trajectory in the horizontal plane for (a) 2 particles and (b) 3 particles.

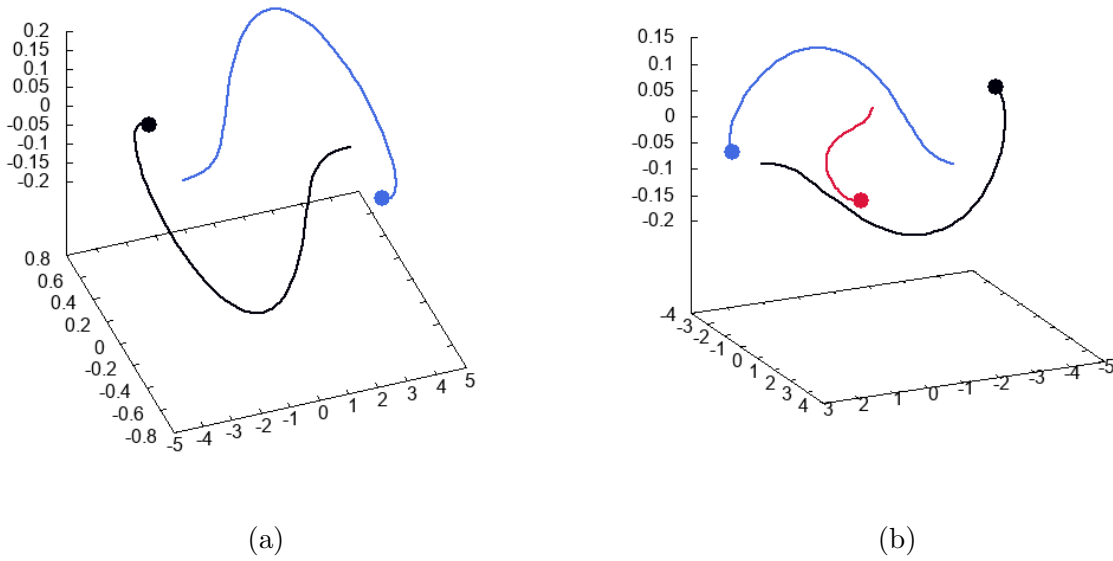


FIGURE 8. **Collision avoidance in 3D.** space trajectories in three dimension for (a) 2 particles and (b) 3 particles.

interactions. We first introduce the point O which represents the point of coordinate x_O defined as

$$\mathbf{x}_O = \arg \min_{\mathbf{x} \in \partial O \cap \mathcal{K}_i(t^0)} d(\mathbf{x}_i(t), \mathbf{x})$$

hence the force field acting on the particle $i \in \{1, \dots, N\}$ is

$$\mathbf{F}^{\text{obs}}(\mathbf{x}_i, \mathbf{v}_i) = \omega_{iO} H(\alpha_{iO}) \mathbf{v}_i \wedge \mathbf{R}_{iO},$$

with $\omega_{iO} > 0$ and a rotation axis \mathbf{R}_{iO} given by

$$\mathbf{R}_{iO} := \frac{\mathbf{v}_i \wedge \mathbf{k}_{iO}}{d_{iO}},$$

with \mathbf{k}_{iO} the unit vector in the direction $\mathbf{x}_O - \mathbf{x}_i$ and $d_{iO} = |\mathbf{x}_O - \mathbf{x}_i|$. The function H_{iO} is given by (2.22) and the frequency $\omega_{iO} > 0$ is

$$\omega_{iO} = \frac{16\pi}{|\mathbf{R}_{iO}|} e^{-\tau_{i0}},$$

with $\tau_{i0} > 0$ given by (2.2).

The particles are attracted to the target $\mathbf{x}_T = (7, 7, 0)$, whereas the obstacles are represented by two balls $B(\mathbf{x}_0, 1/2)$ and $B(\mathbf{x}_1, 1)$ with $\mathbf{x}_0 = (2, 2, 0)$ and $\mathbf{x}_1 = (5, 5, 0)$.

We represent in Figure 9 the space trajectories at different time. The particles are initially located on a sphere centered in $(-1, -1, 0)$ with a random velocity. On the one hand we observe that due to the attractive potential, all particles choose the same direction and thanks to the collision avoidance operator, they do not collide. On the other hand, when they approach the obstacle they deviate and remain relatively far from the obstacles. Finally at time $t = 20$, all particles are moving around the target point.

5. CONCLUSION AND PERSPECTIVES

In this article, we have proposed a three dimensional dynamical model for collision avoidance based on previous works in two dimension for pedestrian flows [9, 10, 28]. This individual based model relies on a vision-based framework: the particles analyze the scene and react to the collision threatening partners by changing their direction of motion. We have also proposed a kinetic version of this individual based model and perform some numerical experiments which illustrate the ability of the microscopic model to avoid collisions in three dimensions.

In a future work, the approach developed in Section 3, which is based on a mean field model, will be investigated to study the collision avoidance process in the presence of many vehicles. Indeed for a large number of particles, sensors are not able to distinguish each individual but only clouds of particles are detected, the application of mean field models may contribute on the design of efficient algorithms since the sum of interacting particles is replaced by a self consistent force.

On the other hand, more precise models can be applied to describe the motion in three dimension of vehicles as multi-agent dynamics where each agent is described by its position and body attitude. More precisely, each agent travels in a given direction and its frame can rotate around it adopting different configurations. In this manner, the frame attitude is described by three orthonormal axes giving rotation matrices [11].

6. ACKNOWLEDGEMENT

The authors thank anonymous referees and highly appreciate their valuable comments and suggestions, which significantly contributed to improve the quality of the justification of the model in Section 2.2.

REFERENCES

- [1] F. BOLLEY, J. A. CANIZO, J. A. CARRILLO, Mean-field limit for the stochastic Vicsek model *Appl. Math. Letters* **25**, pp. 339-343 (2012)
- [2] BONABEAU E., DORIGO M. AND THERAULAZ G. *Swarm Intelligence : From Natural to Artificial Systems Oxford Univ. Press* (1999).
- [3] CAMAZINE, S., DENEUBOURG, J.-L., FRANKS, N. R., SNEYD, J., THERAULAZ, G., AND BONABEAU, E. *Self-Organization in Biological Systems Princeton University Press*, Princeton (2001).
- [4] J. A. CANIZO, J. A. CARRILLO, J. ROSADO, A well-posedness theory in measures for some kinetic models of collective motion, *Math. Mod. Meth. Appl. Sci.* **21**, 515-539, (2011).
- [5] J. A. CARRILLO, Y.-P. CHOI, M. HAURAY, S. SALEM, Mean-field limit for collective behavior models with sharp sensitivity regions, *J. European Math. Soc.* (2017)

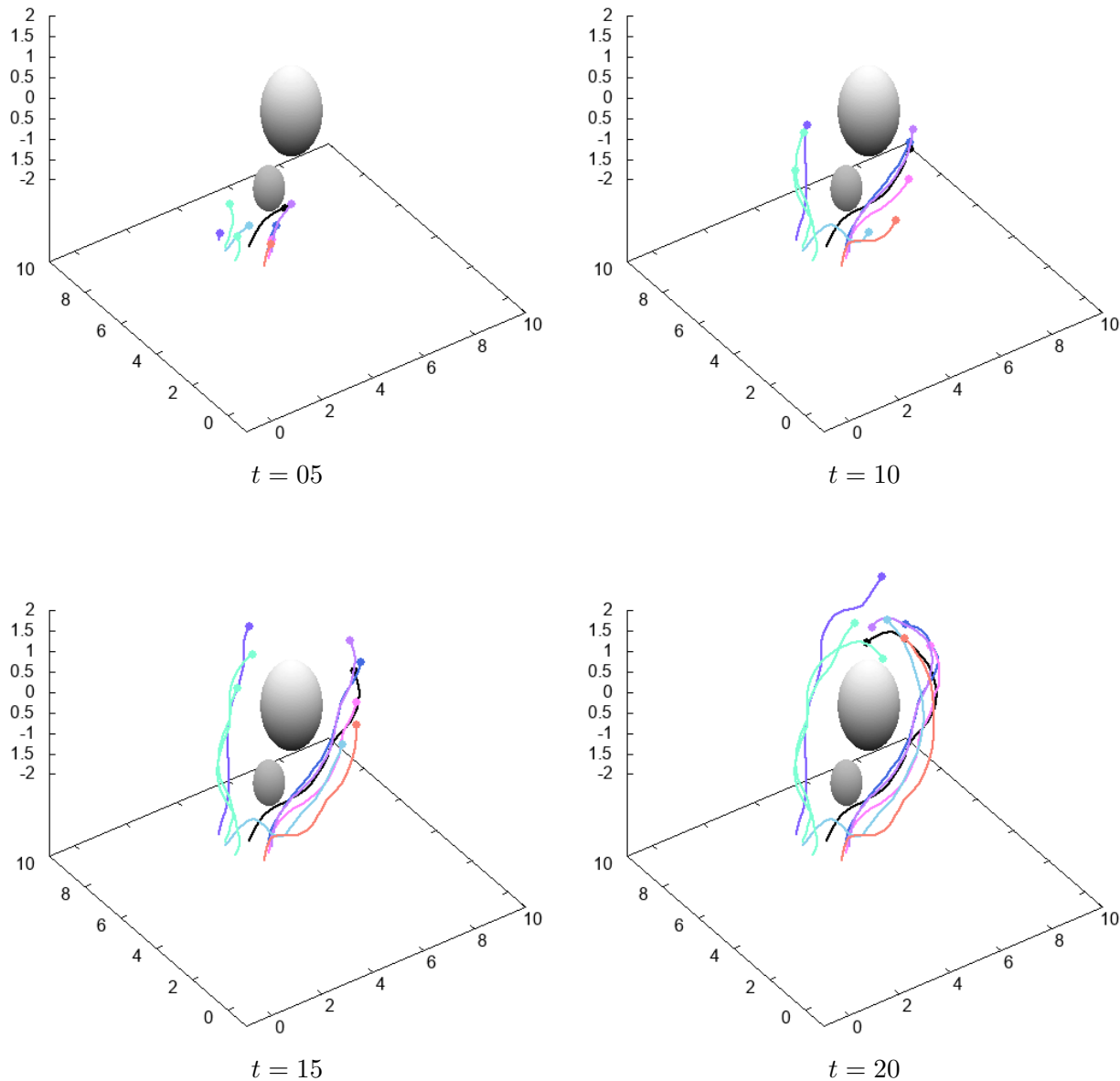


FIGURE 9. **Moving around obstacles.** space trajectory in three dimension at different time $t = 5, 10, 15$ and 20 .

- [6] CARRILLO J.A., FORNASIER M., TOSCANI G., VECIL F. Particle, Kinetic, and Hydrodynamic Models of Swarming. Naldi, G., Pareschi, L., Toscani, G. (eds.) *Mathematical Modeling of Collective Behavior in Socio-Economic and Life Sciences*, Series: Modelling and Simulation in Science and Technology, Birkhauser, (2010), 297-336.
- [7] CARRILLO, JOS A.; KLAR, AXEL; MARTIN, STEPHAN; TIWARI, SUDARSHAN, Self-propelled interacting particle systems with roosting force. *Math. Models Methods Appl. Sci.* **20** (2010), suppl. 1, 15331552.
- [8] CHAKRAVARTHY A. AND GHOSE D., Obstacle avoidance in a dynamic environment: a collision cone approach. *IEEE Transactions on Systems, Man and Cybernetics, Part A: Systems and Humans*, **28**, pp. 562574 (1998).
- [9] DEGOND P., APPERT-ROLLAND C., MOUSSAID M., PETTRE J., THERAULAZ G. Vision-based macroscopic pedestrian models *Kinetic and Related Models*, (2013).
- [10] DEGOND P., APPERT-ROLLAND C., MOUSSAID M., PETTRE J., THERAULAZ G. A Hierarchy of Heuristic-Based Models of Crowd Dynamics *J Stat Phys* **152** pp. 1033-1068, (2013).

- [11] DEGOND P., FROUVELLE A., MERINO-ACEITUNO S., A new flocking model through body attitude coordination. *Mathematical Models and Methods in Applied Sciences* (2017).
- [12] EBY M. S., A self-organizational approach for resolving air traffic conflicts *The Lincoln Laboratory Journal*, **7**, pp. 239254 (1994).
- [13] EBY M. S. AND KELLY W.E., Free flight separation assurance using distributed algorithms *Proceedings of the IEEE Aerospace Conference*, San Francisco, USA, pp. 429441 (1999).
- [14] ETIKYALA, R., GTTLICH, S.; KLAR, A.; TIWARI, S. Particle methods for pedestrian flow models: from microscopic to nonlocal continuum models. *Math. Models Methods Appl. Sci.* **24** (2014), no. 12, 25032523
- [15] ETIKYALA, R.; GTTLICH, S.; KLAR, A.; TIWARI, S. A macroscopic model for pedestrian flow: comparisons with experimental results of pedestrian flow in corridors and T-junctions. *Neural Parallel Sci. Comput.* **22** (2014), no. 3, 315330.
- [16] A. F. FILIPPOV, Differential equations with discontinuous righthand sides, *Differential Equations with Discontinuous Right-Hand Sides. Mathematics and Its Applications*, Kluwer Academic, Dordrecht, (1988).
- [17] FRAICHARD T. AND ASAMA H., Inevitable collision states a step towards safer robots? *Advanced Robotics*, **18**, pp. 10011024 (2004).
- [18] GARCIA G. A., KESHMIRI S. S. Biologically inspired trajectory generation for swarming UAVs using topological distances. *Elsevier Aerospace Science and Technology* **54** 312-319, (2016).
- [19] GIARDINA I. Collective behavior in animal groups: theoretical models and empirical studies *HFSP Journal* **2:205-219** (2008).
- [20] GOLSE F., The mean field limit for the dynamics of large particle systems. *Journées équations aux dérivées partielles*, **9** pp. 1-47, (2003).
- [21] GOMEZ M. L. AND FRAICHARD T., Benchmarking collision avoidance schemes for dynamic environments *Proceedings of the ICRA Workshop on Safe Navigation in Open and Dynamic Environments*, Kobe, Japan (2009).
- [22] HOEKSTRA J., RUIGROK R. C. J. AND VAN GENT R. N. H. W., Free flight in a crowded airspace? *3rd USA/Europe Air Traffic Management RD Seminar*, Napoli, Italy (2000).
- [23] HAN J., XU Y., DI L., AND CHEN Y.Q. Low-cost multi-UAV technologies for contour mapping of nuclear radiation field *J. Intell. Robot. Syst.* **70**, no 1-4, pp. 401-410, (Apr. 2013).
- [24] HSU E. P., Stochastic Analysis on Manifolds, *Graduate Series in Mathematics*, **38**, American Mathematical Society, Providence, Rhode Island, 2002.
- [25] KOPFSTEDT T., MUKAI M., FUJITA M., AND AMENT C. Control of formations of UAVs for surveillance and reconnaissance missions *Proc. 17th IFAC World Congr.* pp. 611, (Jul. 2008).
- [26] LACHER A. R., MARONEY D. R. AND ZEITLIN A. D., Unmanned aircraft collision avoidance: Technology assessment and evaluation methods. *Proceedings of the 7th USA/Europe Air Traffic Management Research and Development Seminar*, Barcelona, Spain (2007).
- [27] B. OKSENDAL, Stochastic Differential Equations: An Introduction with Applications. Springer, New York, 6th edition (2003).
- [28] MOUSSAD M., HELBING D., THERAULAZ G. How simple rules determine pedestrian behavior and crowd disasters. *Proceedings of the National Academy of Science* **108:6884-6888**, (2011).
- [29] PARRISH J. AND EDELSTEIN-KESHET L. Complexity, pattern, and evolutionary trade-offs in animal aggregation, *Science* **294** 99-101 (1999).
- [30] ROELOFSEN S., MARTINOLI A. AND GILLET D. 3D Collision Avoidance Algorithm for Unmanned Aerial Vehicles with Limited Field of View Constraints. Conference on Decision and Control, Las Vegas, Nevada, USA, (2016).
- [31] H. SPOHN, Large scale dynamics of interacting particles, Springer, Berlin, 1991.

CÉLINE PARZANI

ECOLE NATIONALE DE L'AVIATION CIVILE
 LABORATOIRE ENAC, ÉQUIPE OPTIM
 7 AVENUE DOUARD-BELIN,
 BP 54005 TOULOUSE, FRANCE

E-MAIL: celine.parzani@enac.fr

FRANCIS FILBET

UNIVERSITÉ DE TOULOUSE III & IUF
UMR5219, INSTITUT DE MATHÉMATIQUES DE TOULOUSE,
118, ROUTE DE NARBONNE
F-31062 TOULOUSE CEDEX, FRANCE

E-MAIL: francis.filbet@math.univ-toulouse.fr